introduction to nanoelectromechanical systems

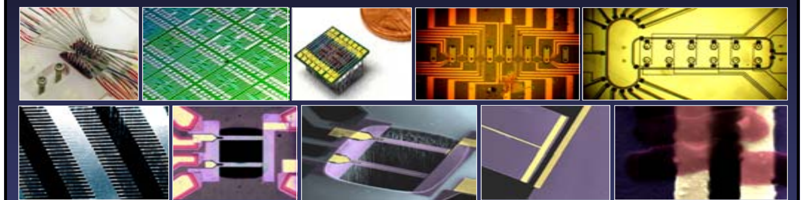

Michael Roukes
Kavli Nanoscience Institute
Physics, Applied Physics, & Bioengineering
California Institute of Technology

NEMS: multiterminal mechanical devices

ELECTRICAL INPUT SIGNAL → input transducer → mechanical stimulus → nano-mechanical system → mechanical response → output transducer → ELECTRICAL OUTPUT SIGNAL

ELECTRICAL CONTROL SIGNAL → control transducer → mechanical perturbation → nano-mechanical system

mechanical domain
- -signal processing
- -measurement / sensing
- -computation

Fundamentals: important concepts

- beam mechanics (review)
- responsivity } sensitivity
- noise } sensitivity
- dynamic range
- nonlinear response

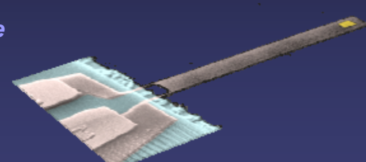

Continuum Solid: Equations of Motion

Isotropic solid with local displacement $\vec{u}(\vec{r},t)$

$$\rho\frac{\partial^2\vec{u}}{\partial t^2}=(\lambda+\mu)\nabla(\nabla\cdot\vec{u})+\mu\nabla^2\vec{u}$$

Young's modulus $E=\dfrac{\mu(3\lambda+2\mu)}{\lambda+\mu}$

λ, μ are the Lamé constants:

$\lambda=c_{12}\quad \mu=c_{44}=(c_{11}-c_{12})/2$

Poisson ratio $\nu=\dfrac{\lambda}{2\lambda+2\mu}$

Boundary conditions define stress or strain:

Fixed boundary: $\vec{u}(\vec{r}_b,t)=0$ for $\vec{r}_b$ on boundary

Stress-free boundary: $\vec{T}(\vec{r}_b,t)\cdot\hat{n}=0$ for $\vec{r}_b$ on boundary, $\hat{n}$ unit normal

$$T_{ii}=(\lambda+2\mu)\nabla\cdot\vec{u}$$

$$T_{ij}=\mu\left(\frac{\partial u_i}{\partial r_j}+\frac{\partial u_j}{\partial r_i}\right)$$

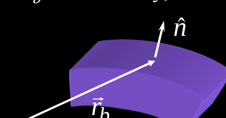

see Auld, *Acoustic Waves and Fields in Solids* (2nd ed.) 1990

 Ph/EE 118c, Ch227 — Micro- and Nanoscale Sensors

Flexural Beams: Equations of Motion

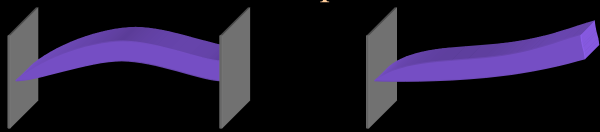

Euler-Bernoulli theory: ***length >> width, thickness***

- Neutral axis displacement Y
- Width w, thickness t (along y)
- Density ρ, modulus $E = (3\lambda+2\mu)/(\lambda+\mu)$

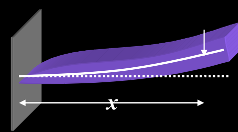

$$\rho w t \frac{\partial^2 Y}{\partial t^2} + E\frac{wt^3}{12}\frac{\partial^4 Y}{\partial x^4} = 0$$

Boundaries: Clamped end: $Y = 0$, $Y' = 0$ Free end: $Y'' = 0$, $Y''' = 0$

See Timoshenko, *Vibration Problems in Engineering* (1974)

 Ph/EE 118c, Ch227 — Micro- and Nanoscale Sensors

Flexural Beams: Solutions

$$Y_n(x,t) = a_n(\cos\beta_n x - \cosh\beta_n x) + b_n(\sin\beta_n x - \sinh\beta_n x)$$

Doubly-clamped beam

$a_n \approx b_n \; (a_1 = 1.018 b_1, a_2 = 0.9992 b_2, a_3 = 1.000 b_3 \ldots)$

$\beta_n L = 4.730, 7.853, 10.996\ldots$

$\omega_n = \sqrt{E/12\rho}\,\beta_n t$

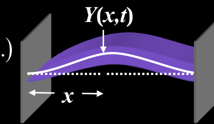

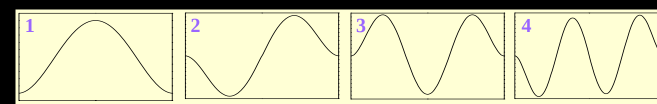

 Ph/EE 118c, Ch227 — Micro- and Nanoscale Sensors

Flexural Beams: Solutions

$$Y_n(x,t) = a_n(\cos\beta_n x - \cosh\beta_n x) + b_n(\sin\beta_n x - \sinh\beta_n x)$$

Cantilevered beam

$a_n \approx -b_n \; (a_1 = -1.362 b_1, a_2 = -0.982 b_2, a_3 = -1.008 b_3 \ldots)$

$\beta_n L = 1.875, 4.694, 7.855\ldots$

$\omega_n = \sqrt{E/12\rho}\,\beta_n t$

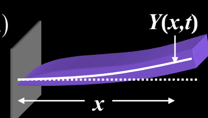

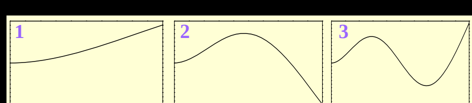

 Ph/EE 118c, Ch227 — Micro- and Nanoscale Sensors

Flexural Beams: *Damped Harmonic Motion*

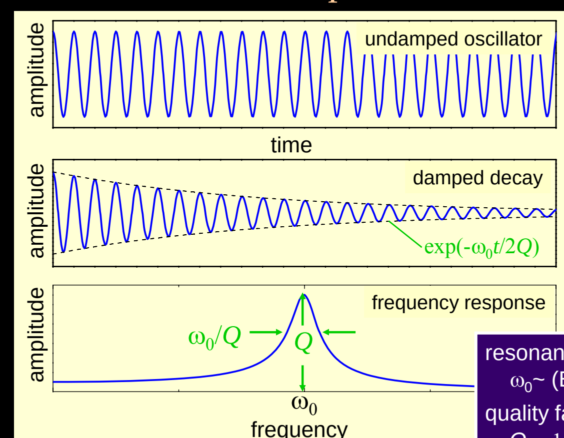

resonance frequency: $\omega_0 \sim (E_{eff}/\rho)^{1/2}$

quality factor: $Q \sim 1/\Delta$

 Ph/EE 118c, Ch227 — Micro- and Nanoscale Sensors

Single Mode Model: Damped SHO

A damped, simple harmonic oscillator model describes the flexural motion of a beam in the vicinity of the fundamental resonance with an accuracy to within 1% for Q>10.

displacement — applied force

complex displacement response function: $$\tilde{x}(\omega) = \frac{\tilde{F}(\omega)}{[K - \omega^2 M_{eff}] - i\omega\gamma_{eff}(\omega)}$$

force constant

comments:

- this is a "dynamical version" of Hooke's law $x = F_{applied}/k$
- the complex AC mechanical responsivity is defined as $\tilde{x}(\omega) = \Re(\omega)\tilde{F}(\omega)$,

  i.e. $\Re(\omega) = \frac{1}{[K - \omega^2 M_{eff}] - i\omega\gamma_{eff}(\omega)}$

Parameters:

effective mass, M_{eff}

dynamic stiffness (for point loading at beam's center), K_{eff}

quality factor, Q

© M.L. Roukes 2005 Ph/EE 118c, Ch227 — Micro- and Nanoscale Sensors

Single Mode Model: Damped SHO

A damped, simple harmonic oscillator model describes the flexural motion of a beam in the vicinity of the fundamental resonance with an accuracy to within 1% for Q>10.

displacement — applied force

complex displacement response function: $$\tilde{x}(\omega) = \frac{\tilde{F}(\omega)}{[K - \omega^2 M_{eff}] - i\omega\gamma_{eff}(\omega)}$$

force constant

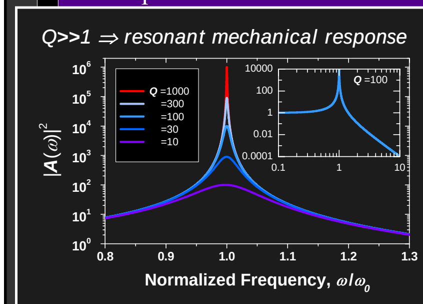

Parameters:

effective mass, M_{eff}

dynamic stiffness (for point loading at beam's center), K_{eff}

quality factor, Q

Ph/EE 118c, Ch227 — Micro- and Nanoscale Sensors

Single Mode Model: Damped SHO

A damped, simple harmonic oscillator model describes the flexural motion of a beam in the vicinity of the fundamental resonance with an accuracy to within 1% for Q>10.

displacement response function: $$\tilde{x}(\omega) = \frac{\tilde{F}(\omega)}{[K - \omega^2 M_{eff}(\omega)] - i\omega\gamma_{eff}(\omega)}$$

For the *fundamental*-mode response of a simple doubly-clamped beam,

effective mass: $M_{eff} = 0.735 l t w \rho$

dynamic stiffness: $\kappa_{eff} = 32 E t^3 w / l^3$

resonance frequency: $\omega_0 = 2\pi(1.05)\sqrt{E/\rho}\,(t/l^2)$

N.B. For this simple treatment of beam elasticity, all of these factors apply only to the specific mode considered.

Here, $l \times t \times w$ are the beam's dimensions, E is Young's modulus and ρ is the mass density of the beam. The above assumes the material is isotropic; for single-crystal devices anisotropy in the elastic constants yields resonance frequency dependence upon crystallographic orientation.

© M.L. Roukes 2005 Ph/EE 118c, Ch227 — Micro- and Nanoscale Sensors

Single Mode Model: *Cantilever DSHO*

Resonance frequency (cantilever): $\frac{\omega_0}{2\pi} = 0.159\sqrt{\frac{E_{eff}}{\rho}}\frac{t}{L^2}$

eff. force constant (cantilever): $K_{eff} = (0.2575)\, E \left(\frac{t}{L}\right)^3 w$

Dissipation: Q^{-1}

Effective mass: $M_{eff} = k_{eff} / \omega_0^2$

DC Response: $\Delta Y = F / K_{eff}$ (*constant force*)

Resonant response: $\Delta Y = Q F / K_{eff}$ (*at* ω_0)

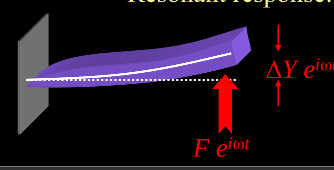

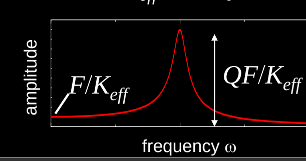

© M.L. Roukes 2005 Ph/EE 118c, Ch227 — Micro- and Nanoscale Sensors

3

Fluctuation-Dissipation Theorem: Thermomechanical Noise

Thermal force spectral density associated with finite Q:

$$S_F(\nu) = 4k_B T_N \frac{k_{eff}}{\omega_0 Q} \qquad T_N = \text{noise temperature}$$

Displacement spectral density $S_x(\omega)$ for force density $S_F(\omega)$

$$S_x(\omega) = |\Re|^2 S_F(\omega) = \frac{\omega_0}{QM_{eff}} \frac{4k_B T_N}{(\omega_0^2 - \omega^2)^2 + \left(\frac{\omega\omega_0}{Q}\right)^2}$$

This yields thermal equilibrium of the average total energy:

$$\langle E \rangle = \langle T + U \rangle = k_B T_N$$

 Ph/EE 118c, Ch227 — Micro- and Nanoscale Sensors

Displacement and Force Noise

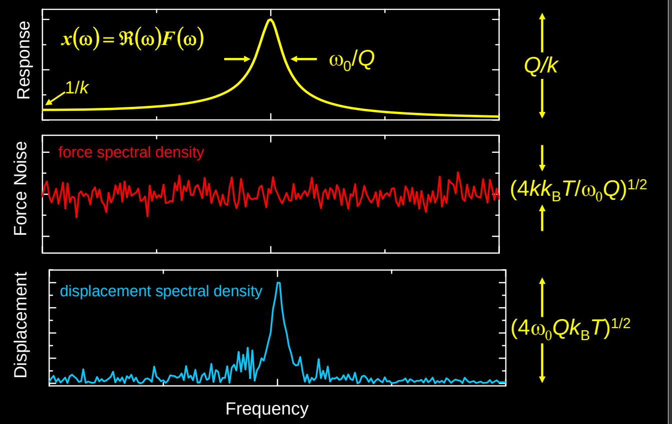

 Ph/EE 118c, Ch227 — Micro- and Nanoscale Sensors

Displacement and Force Noise

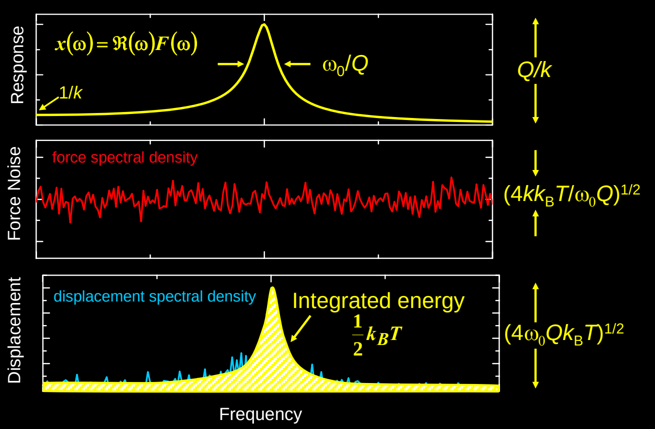

 Ph/EE 118c, Ch227 — Micro- and Nanoscale Sensors

The two key attributes for sensing:

- **responsivity**
  metric quantifying *transduction* (conversion between signal domains; generalization of "gain")
- **noise**
  imposes minimum detectable signal level; each element of a system degrades the overall SNR (signal-to-noise ratio).

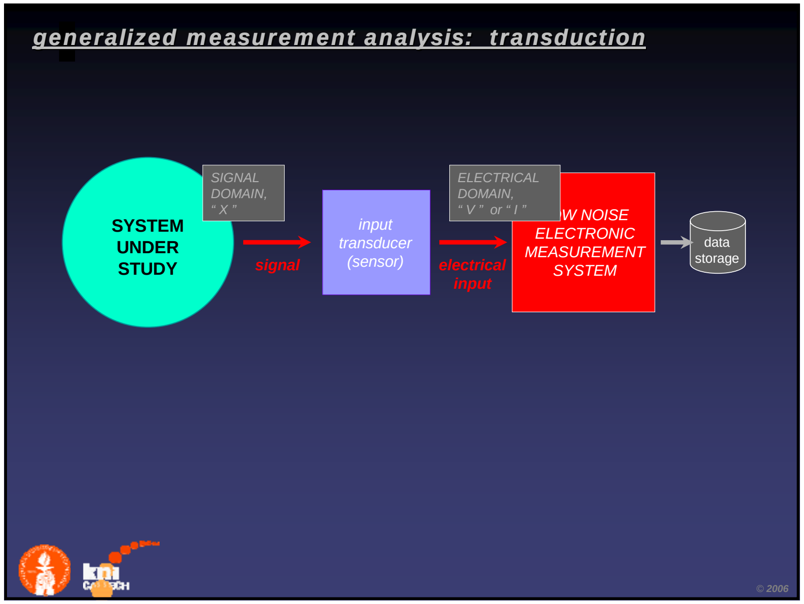
generalized measurement analysis: transduction
SYSTEM UNDER STUDY
SIGNAL DOMAIN, " X "
signal
input transducer (sensor)
ELECTRICAL DOMAIN, " V " or " I "
electrical input
W NOISE ELECTRONIC MEASUREMENT SYSTEM
data storage
© 2006

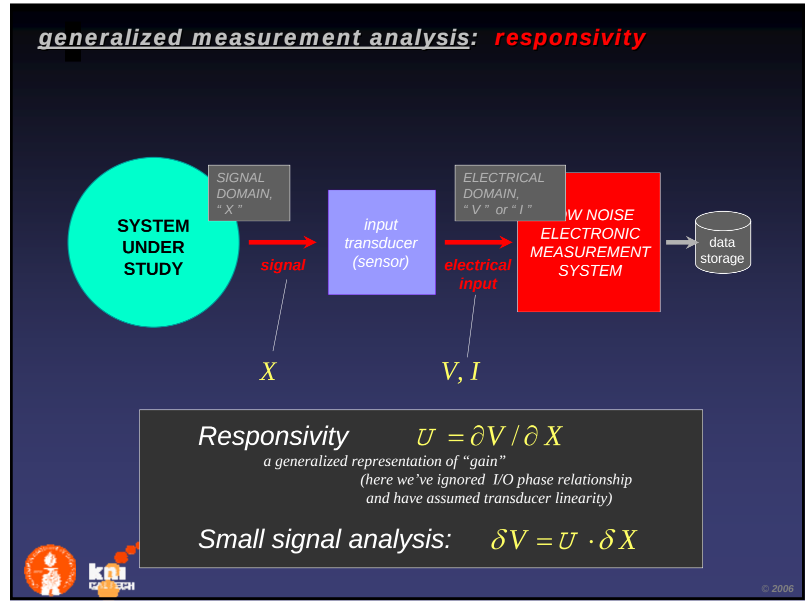
generalized measurement analysis: responsivity
SYSTEM UNDER STUDY
SIGNAL DOMAIN, " X "
signal
input transducer (sensor)
ELECTRICAL DOMAIN, " V " or " I "
electrical input
W NOISE ELECTRONIC MEASUREMENT SYSTEM
data storage
X
V, I
Responsivity $\mathcal{U} = \partial V / \partial X$
a generalized representation of "gain"
(here we've ignored I/O phase relationship and have assumed transducer linearity)
Small signal analysis: $\delta V = \mathcal{U} \cdot \delta X$
© 2006

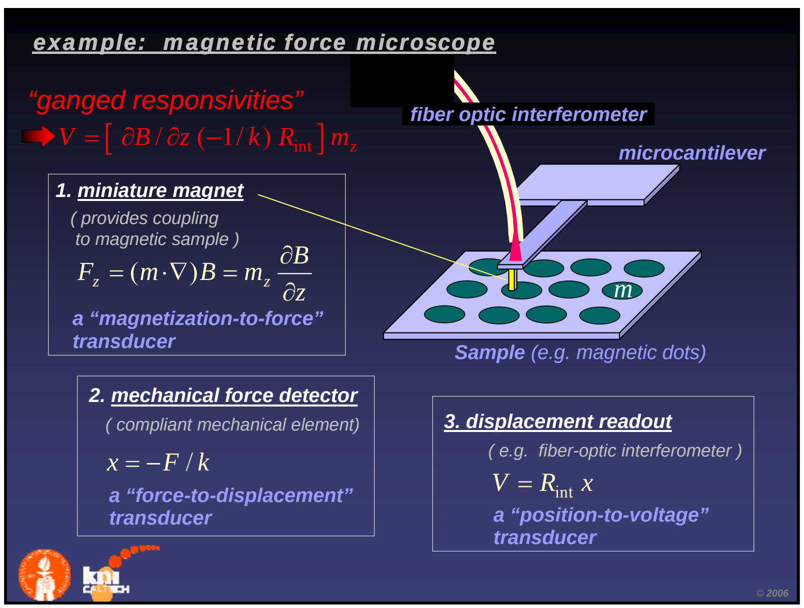
example: magnetic force microscope
"ganged responsivities"
$V = [\, \partial B / \partial z \, (-1/k) \, R_{int} \,] \, m_z$
fiber optic interferometer
microcantilever
1. miniature magnet
(provides coupling to magnetic sample)
$F_z = (m \cdot \nabla) B = m_z \dfrac{\partial B}{\partial z}$
a "magnetization-to-force" transducer
m
Sample (e.g. magnetic dots)
2. mechanical force detector
(compliant mechanical element)
$x = -F / k$
a "force-to-displacement" transducer
3. displacement readout
(e.g. fiber-optic interferometer)
$V = R_{int} \, x$
a "position-to-voltage" transducer
© 2006

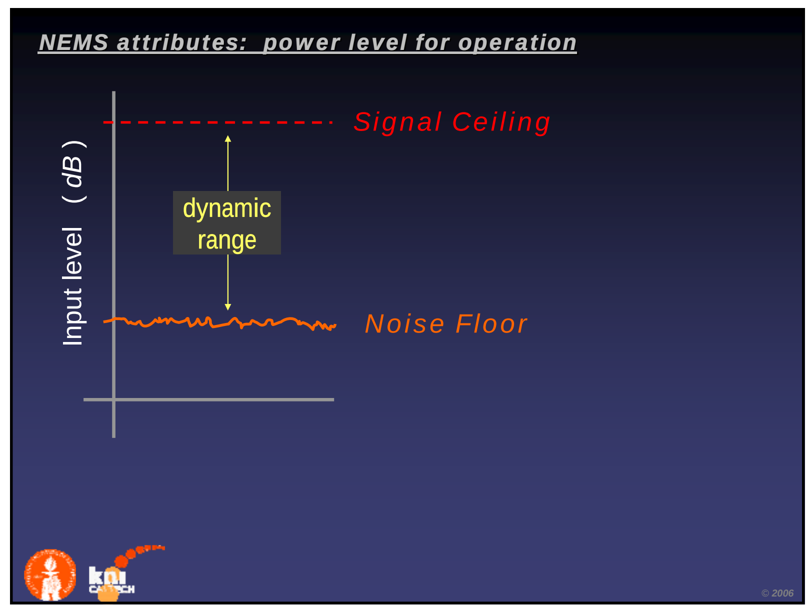
NEMS attributes: power level for operation
Signal Ceiling
dynamic range
Noise Floor
Input level (dB)
© 2006

NEMS attributes: power level for operation

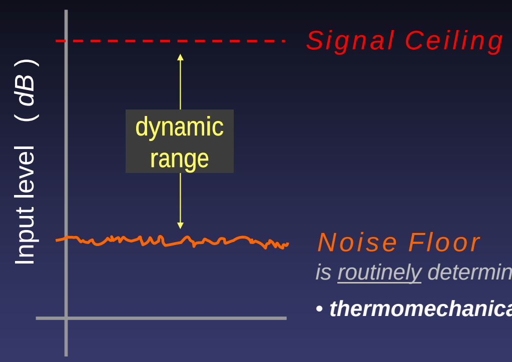

Noise Floor

is routinely determined by

- ***thermomechanical noise***

but, in certain systems (at millikelvin temperatures) *is now approaching:*

- ***quantum displacement fluctuations*** (lecture 2)

"thermomechanical" noise floor

- **fundamental thermodynamic noise limit**

"displacement noise spectral density" units: [(nm)²/Hz]

$$S_x = \frac{4 k_B T Q}{k \omega_0}$$

on resonance

Q>>1 ⇒ resonant mechanical response

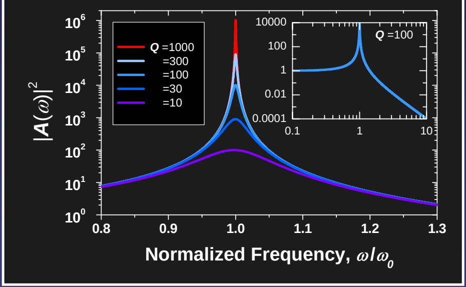

"thermomechanical" noise floor

- **fundamental thermodynamic noise limit**

"displacement noise spectral density" units: [(nm)²/Hz]

$$S_x = \frac{4 k_B T Q}{k \omega_0}$$

on resonance

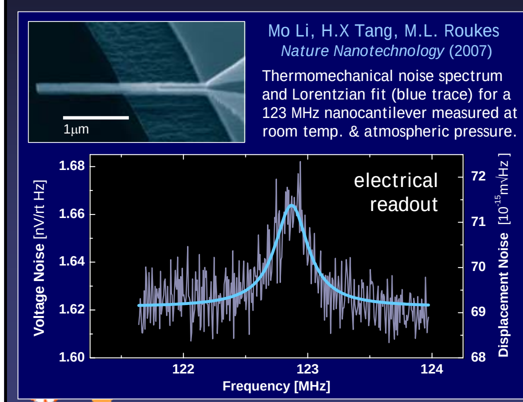

Mo Li, H.X Tang, M.L. Roukes *Nature Nanotechnology* (2007)

Thermomechanical noise spectrum and Lorentzian fit (blue trace) for a 123 MHz nanocantilever measured at room temp. & atmospheric pressure.

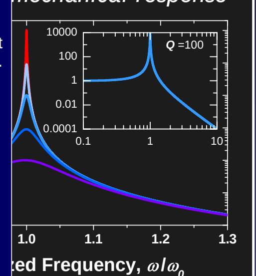

NEMS attributes: power level for operation

nm-Scale Mechanical Resonators

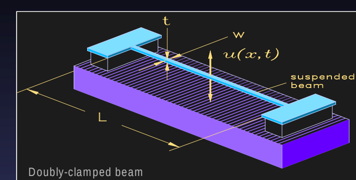

ultralow operating power required (T=300K)

$P_{min} = E_{min} / \tau^*$
$= (k_B T) / (Q/\omega_0)$

f_0	Q	P_{min}	$10^6 \cdot P_{min}$
100 MHz	10,000	40 aW	40 pW
"	100,000	4 aW	4 pW
1 GHz	10,000	0.4 fW	0.4 nW
"	100,000	40 aW	40 pW

- even 10^6 ($10^6 \cdot P_{min}$) ~ μwatts << watts (digital electronics)

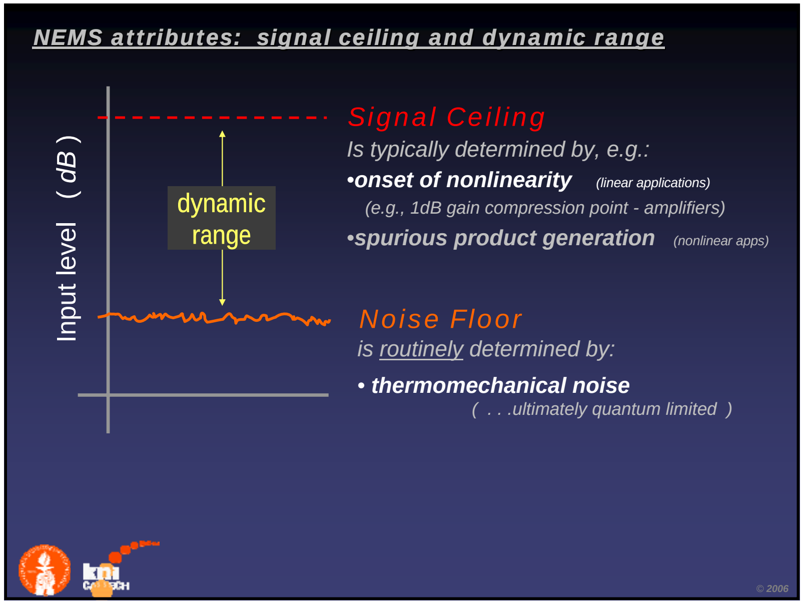
NEMS attributes: signal ceiling and dynamic range
Input level (dB)
dynamic range
Signal Ceiling
Is typically determined by, e.g.:
•onset of nonlinearity (linear applications)
(e.g., 1dB gain compression point - amplifiers)
•spurious product generation (nonlinear apps)
Noise Floor
is routinely determined by:
• thermomechanical noise
(. . .ultimately quantum limited)

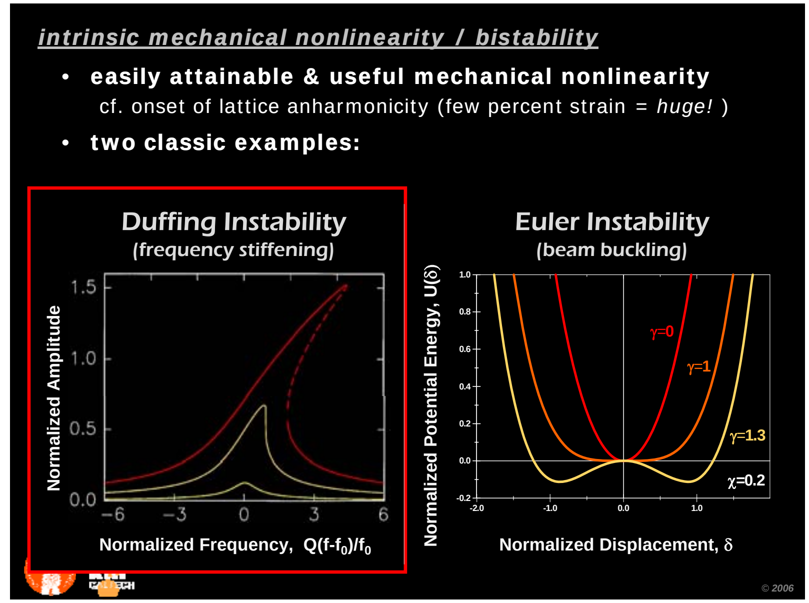
intrinsic mechanical nonlinearity / bistability
• easily attainable & useful mechanical nonlinearity
cf. onset of lattice anharmonicity (few percent strain = huge!)
• two classic examples:
Duffing Instability
(frequency stiffening)
Normalized Amplitude
1.5
1.0
0.5
0.0
−6 −3 0 3 6
Normalized Frequency, $Q(f-f_0)/f_0$
Euler Instability
(beam buckling)
Normalized Potential Energy, U(δ)
γ=0
γ=1
γ=1.3
χ=0.2
Normalized Displacement, δ

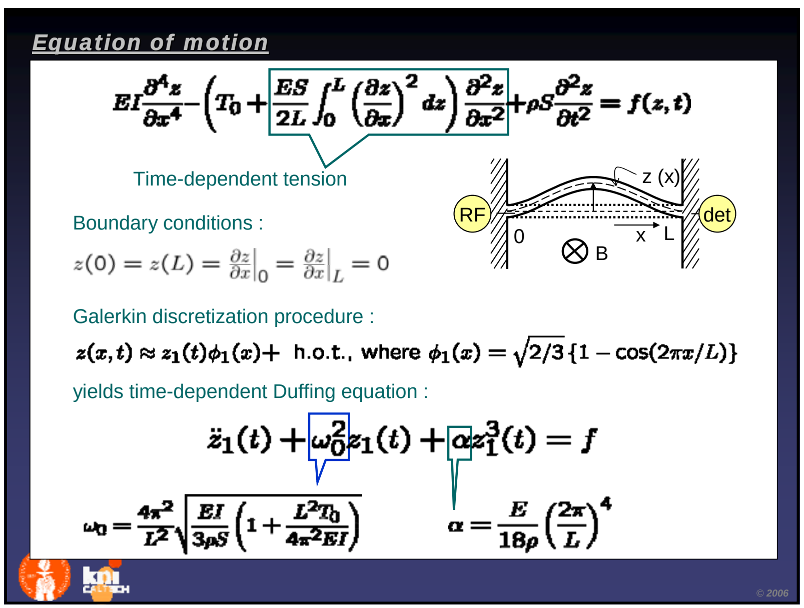
Equation of motion
$$EI\frac{\partial^4 z}{\partial x^4}-\left(T_0+\frac{ES}{2L}\int_0^L\left(\frac{\partial z}{\partial x}\right)^2 dz\right)\frac{\partial^2 z}{\partial x^2}+\rho S\frac{\partial^2 z}{\partial t^2}=f(z,t)$$
Time-dependent tension
RF
det
z (x)
0
x
L
B
Boundary conditions :
$z(0)=z(L)=\frac{\partial z}{\partial x}\Big|_0=\frac{\partial z}{\partial x}\Big|_L=0$
Galerkin discretization procedure :
$z(x,t)\approx z_1(t)\phi_1(x)+$ h.o.t., where $\phi_1(x)=\sqrt{2/3}\{1-\cos(2\pi x/L)\}$
yields time-dependent Duffing equation :
$$\ddot{z}_1(t)+\omega_0^2 z_1(t)+\alpha z_1^3(t)=f$$
$$\omega_0=\frac{4\pi^2}{L^2}\sqrt{\frac{EI}{3\rho S}\left(1+\frac{L^2 T_0}{4\pi^2 EI}\right)}$$
$$\alpha=\frac{E}{18\rho}\left(\frac{2\pi}{L}\right)^4$$

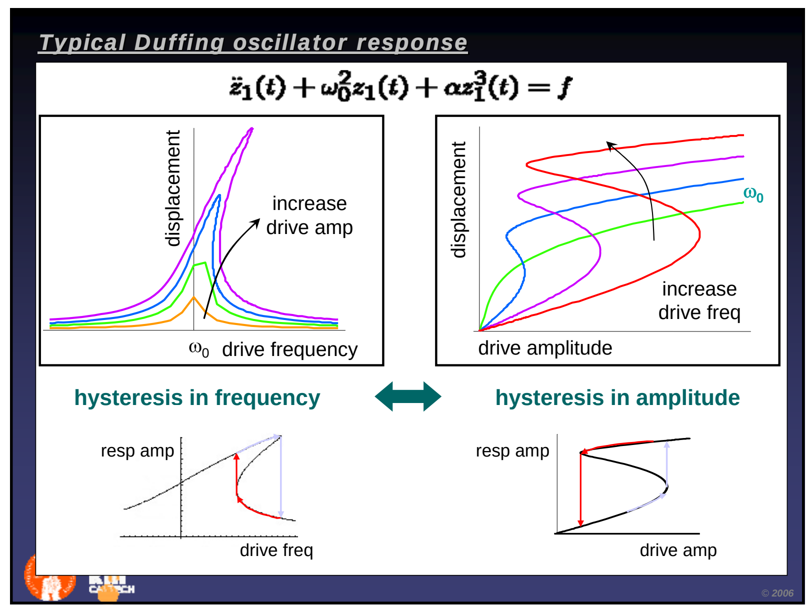
Typical Duffing oscillator response
$$\ddot{z}_1(t)+\omega_0^2 z_1(t)+\alpha z_1^3(t)=f$$
displacement
increase drive amp
ω_0 drive frequency
displacement
ω_0
increase drive freq
drive amplitude
hysteresis in frequency
hysteresis in amplitude
resp amp
drive freq
resp amp
drive amp

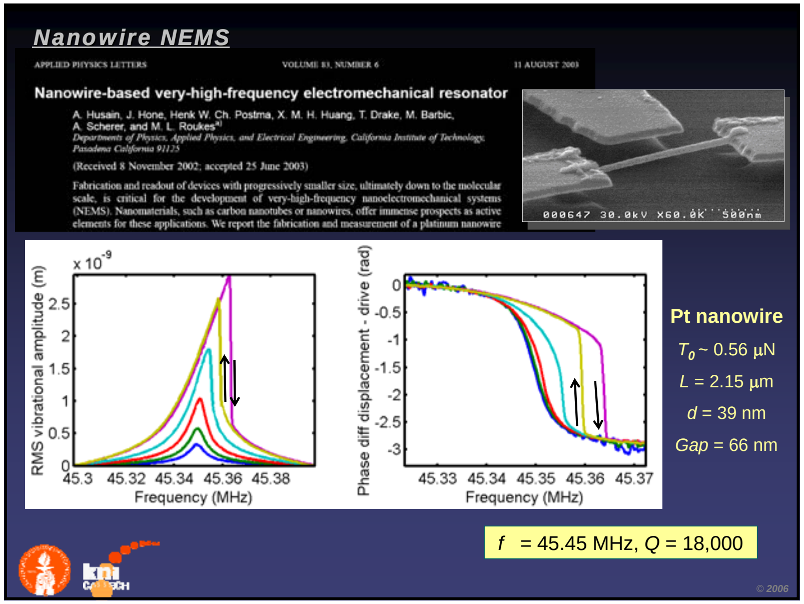
Nanowire NEMS
APPLIED PHYSICS LETTERS VOLUME 83, NUMBER 6 11 AUGUST 2003
Nanowire-based very-high-frequency electromechanical resonator
A. Husain, J. Hone, Henk W. Ch. Postma, X. M. H. Huang, T. Drake, M. Barbic, A. Scherer, and M. L. Roukes
Departments of Physics, Applied Physics, and Electrical Engineering, California Institute of Technology, Pasadena California 91125
(Received 8 November 2002; accepted 25 June 2003)
Fabrication and readout of devices with progressively smaller size, ultimately down to the molecular scale, is critical for the development of very-high-frequency nanoelectromechanical systems (NEMS). Nanomaterials, such as carbon nanotubes or nanowires, offer immense prospects as active elements for these applications. We report the fabrication and measurement of a platinum nanowire
RMS vibrational amplitude (m)
x 10^-9
Frequency (MHz)
Phase diff displacement - drive (rad)
Frequency (MHz)
Pt nanowire
T_0 ~ 0.56 μN
L = 2.15 μm
d = 39 nm
Gap = 66 nm
f = 45.45 MHz, Q = 18,000

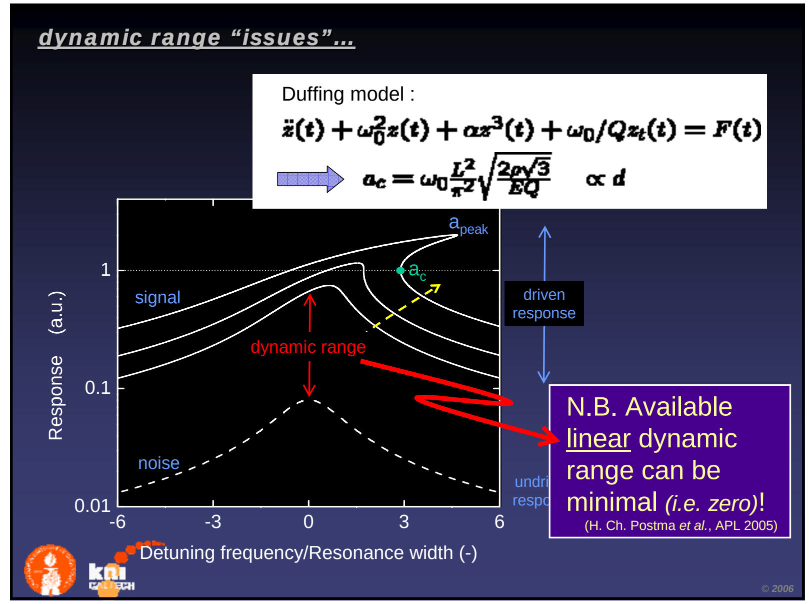
dynamic range "issues"...
Duffing model :
$\ddot{z}(t) + \omega_0^2 z(t) + \alpha z^3(t) + \omega_0/Q\, \dot{z}_t(t) = F(t)$
$a_c = \omega_0 \frac{L^2}{\pi^2}\sqrt{\frac{2\rho\sqrt{3}}{EQ}} \propto d$
Response (a.u.)
a_peak
a_c
signal
dynamic range
noise
driven response
N.B. Available linear dynamic range can be minimal (i.e. zero)!
(H. Ch. Postma et al., APL 2005)
Detuning frequency/Resonance width (-)

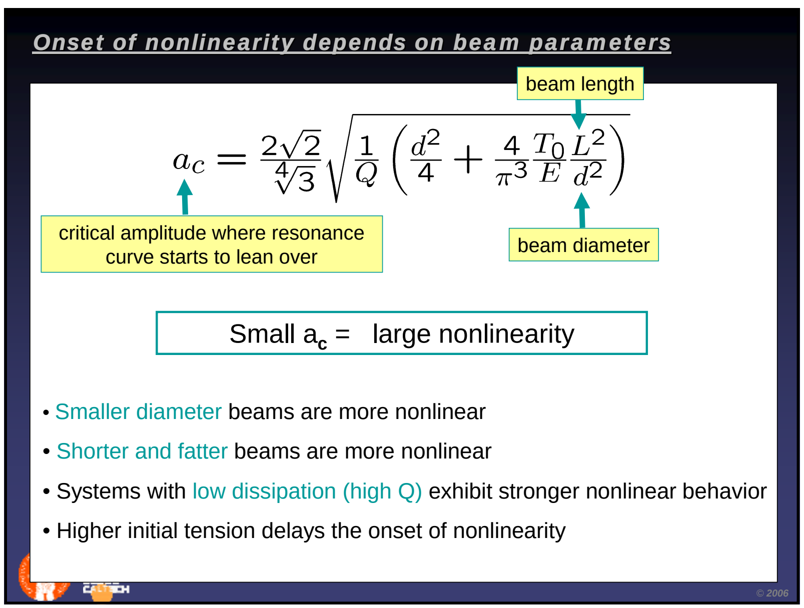
Onset of nonlinearity depends on beam parameters
beam length
$a_c = \frac{2\sqrt{2}}{\sqrt[4]{3}}\sqrt{\frac{1}{Q}\left(\frac{d^2}{4} + \frac{4}{\pi^3}\frac{T_0}{E}\frac{L^2}{d^2}\right)}$
critical amplitude where resonance curve starts to lean over
beam diameter
Small a_c = large nonlinearity
• Smaller diameter beams are more nonlinear
• Shorter and fatter beams are more nonlinear
• Systems with low dissipation (high Q) exhibit stronger nonlinear behavior
• Higher initial tension delays the onset of nonlinearity

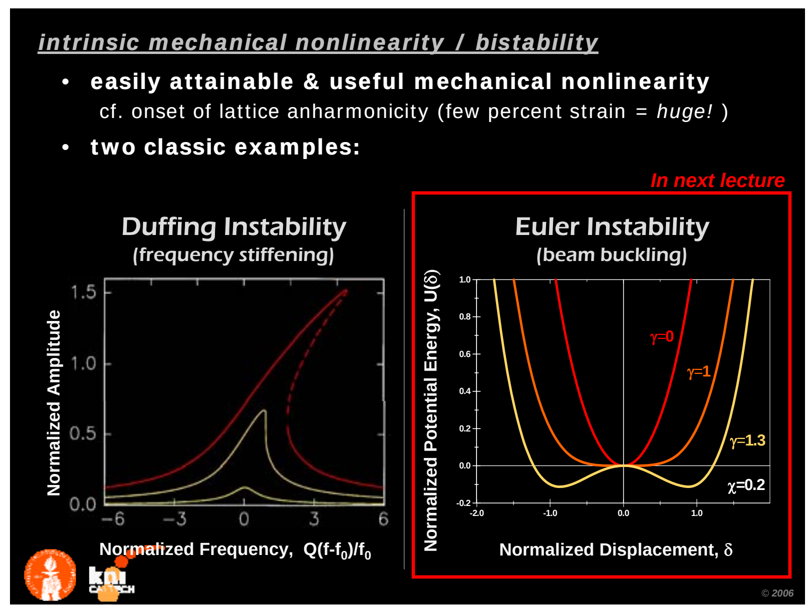
intrinsic mechanical nonlinearity / bistability
• easily attainable & useful mechanical nonlinearity
cf. onset of lattice anharmonicity (few percent strain = huge!)
• two classic examples:
In next lecture
Duffing Instability (frequency stiffening)
Normalized Amplitude
Normalized Frequency, Q(f-f0)/f0
Euler Instability (beam buckling)
Normalized Potential Energy, U(δ)
γ=0
γ=1
γ=1.3
χ=0.2
Normalized Displacement, δ

8

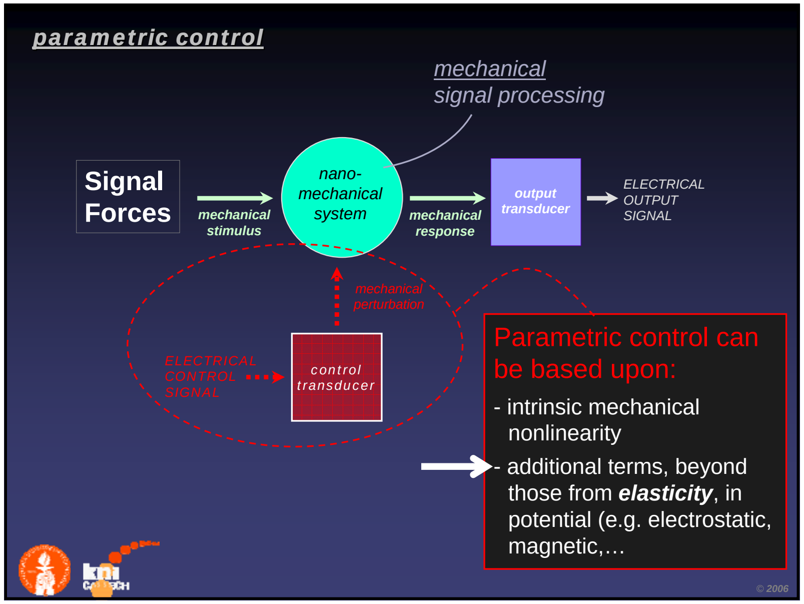
parametric control
mechanical
signal processing
Signal Forces
mechanical stimulus
nano-mechanical system
mechanical response
output transducer
ELECTRICAL OUTPUT SIGNAL
mechanical perturbation
ELECTRICAL CONTROL SIGNAL
control transducer
Parametric control can be based upon:
- intrinsic mechanical nonlinearity
- additional terms, beyond those from elasticity, in potential (e.g. electrostatic, magnetic,…
© 2006

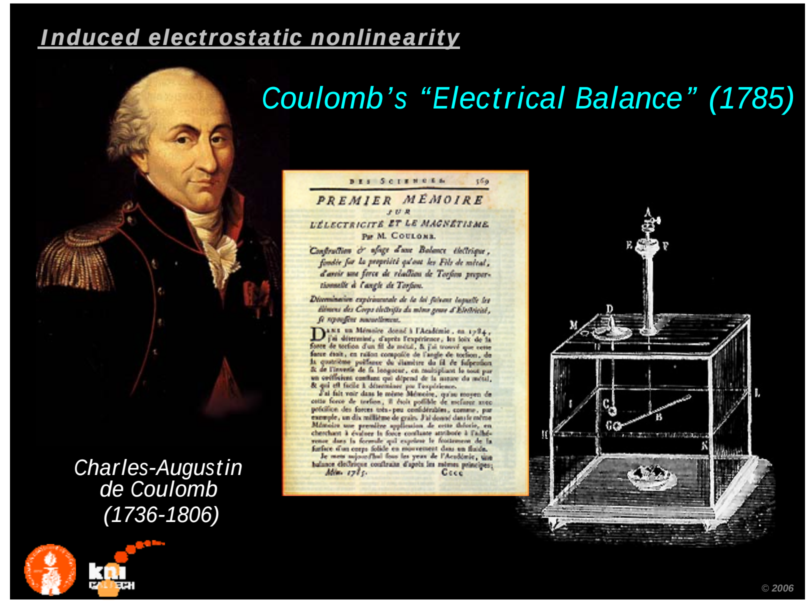
Induced electrostatic nonlinearity
Coulomb's "Electrical Balance" (1785)
PREMIER MÉMOIRE
Charles-Augustin de Coulomb (1736-1806)
© 2006

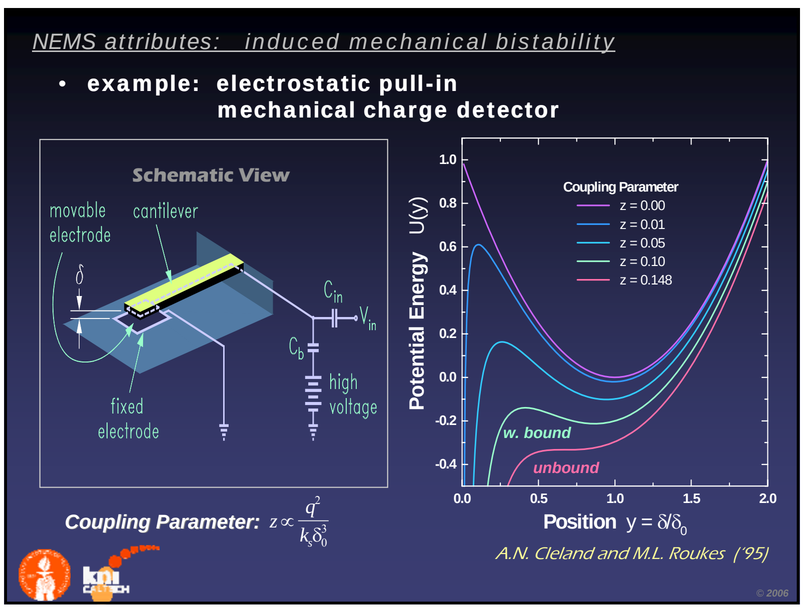
NEMS attributes: induced mechanical bistability
• example: electrostatic pull-in mechanical charge detector
Schematic View
movable electrode
cantilever
δ
C_{in}
V_{in}
C_b
high voltage
fixed electrode
Potential Energy U(y)
Coupling Parameter
z = 0.00
z = 0.01
z = 0.05
z = 0.10
z = 0.148
w. bound
unbound
Position $y = \delta/\delta_0$
Coupling Parameter: $z \propto \frac{q^2}{k_s \delta_0^3}$
A.N. Cleland and M.L. Roukes ('95)
© 2006

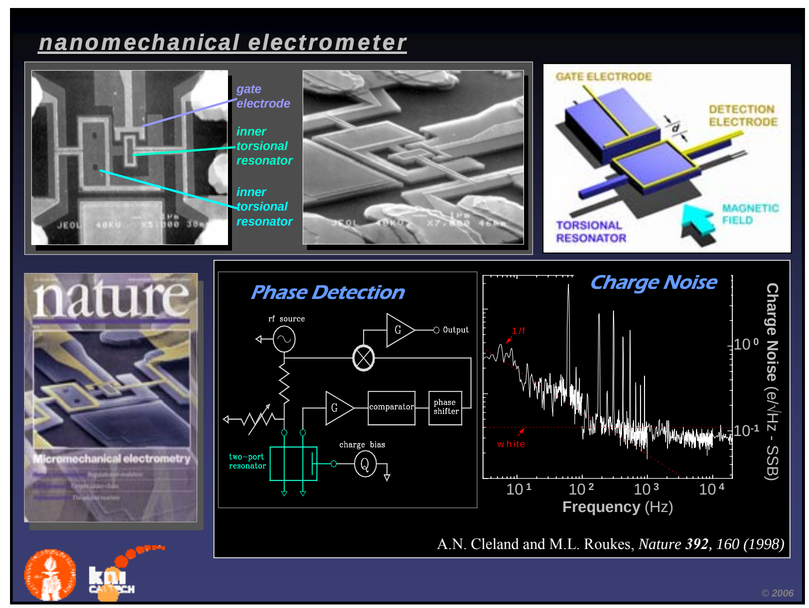
nanomechanical electrometer
gate electrode
inner torsional resonator
inner torsional resonator
GATE ELECTRODE
DETECTION ELECTRODE
TORSIONAL RESONATOR
MAGNETIC FIELD
nature
Micromechanical electrometry
Phase Detection
rf source
Output
comparator
phase shifter
charge bias
two-port resonator
Charge Noise
1/f
white
Frequency (Hz)
Charge Noise (e/√Hz - SSB)
A.N. Cleland and M.L. Roukes, Nature 392, 160 (1998)
© 2006

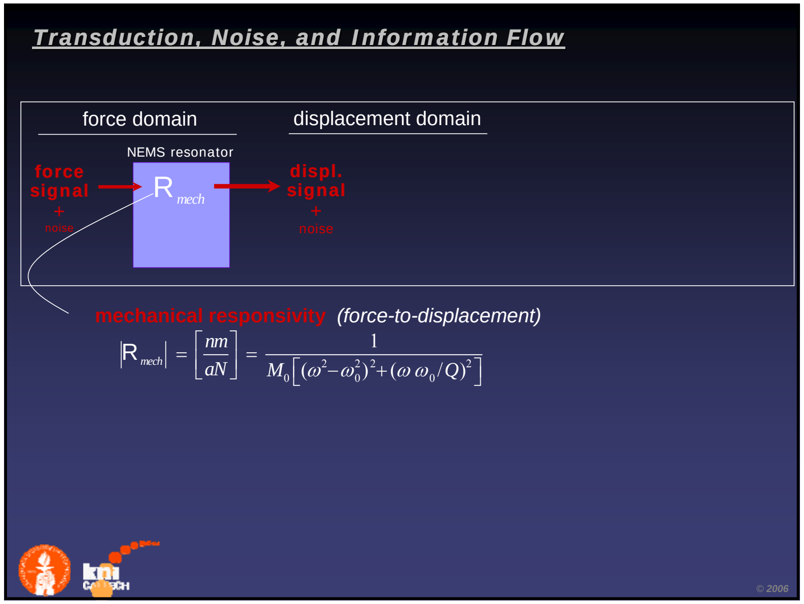
Transduction, Noise, and Information Flow
force domain
displacement domain
NEMS resonator
force signal + noise
R_{mech}
displ. signal + noise
mechanical responsivity (force-to-displacement)
$|R_{mech}| = \left[\frac{nm}{aN}\right] = \frac{1}{M_0\left[(\omega^2-\omega_0^2)^2+(\omega\,\omega_0/Q)^2\right]}$
© 2006

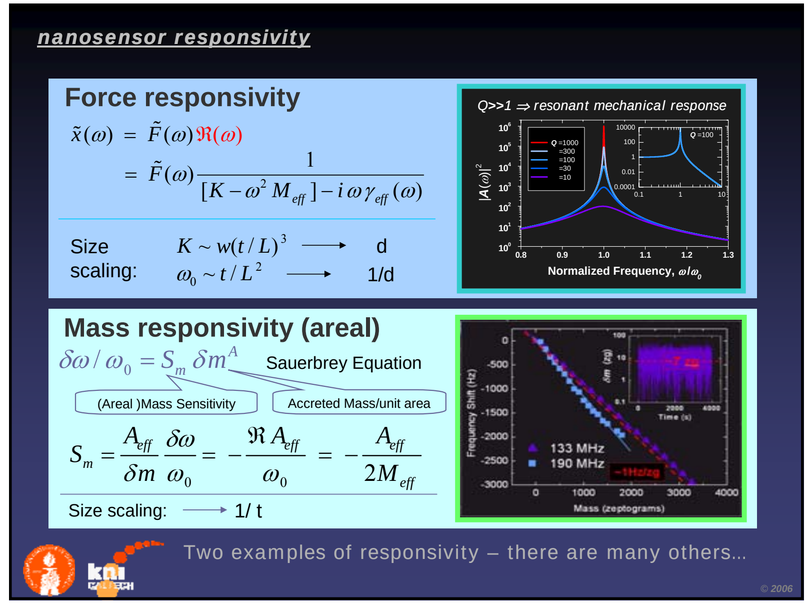
nanosensor responsivity
Force responsivity
$\tilde{x}(\omega) = \tilde{F}(\omega)\Re(\omega)$
$= \tilde{F}(\omega)\frac{1}{[K-\omega^2 M_{eff}]-i\omega\gamma_{eff}(\omega)}$
Size scaling: $K \sim w(t/L)^3 \longrightarrow d$
$\omega_0 \sim t/L^2 \longrightarrow 1/d$
Q>>1 ⇒ resonant mechanical response
Normalized Frequency, ω/ω_0
Mass responsivity (areal)
$\delta\omega/\omega_0 = S_m\,\delta m^A$ Sauerbrey Equation
(Areal)Mass Sensitivity
Accreted Mass/unit area
$S_m = \frac{A_{eff}}{\delta m}\frac{\delta\omega}{\omega_0} = -\frac{\Re A_{eff}}{\omega_0} = -\frac{A_{eff}}{2M_{eff}}$
Size scaling: → 1/ t
133 MHz
190 MHz
Frequency Shift (Hz)
Mass (zeptograms)
Two examples of responsivity – there are many others...
© 2006

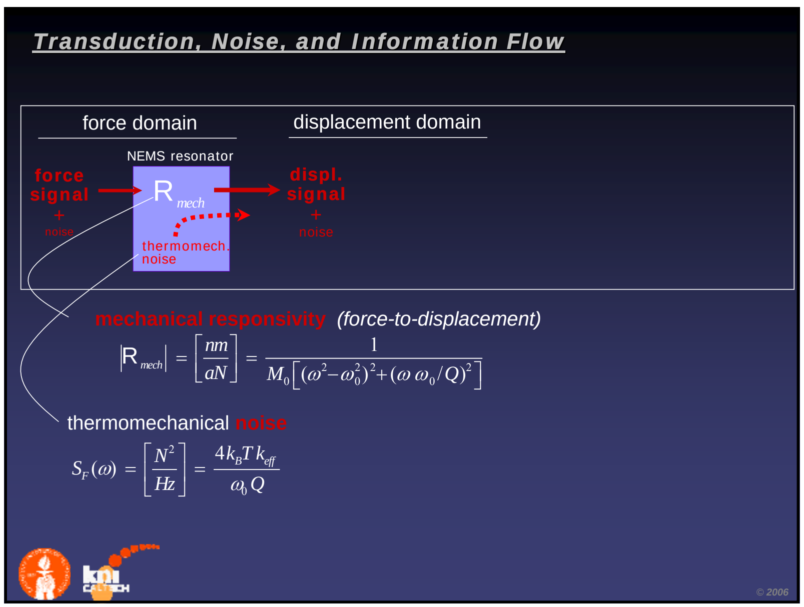
Transduction, Noise, and Information Flow
force domain
displacement domain
NEMS resonator
force signal + noise
R_{mech}
thermomech. noise
displ. signal + noise
mechanical responsivity (force-to-displacement)
$|R_{mech}| = \left[\frac{nm}{aN}\right] = \frac{1}{M_0\left[(\omega^2-\omega_0^2)^2+(\omega\,\omega_0/Q)^2\right]}$
thermomechanical noise
$S_F(\omega) = \left[\frac{N^2}{Hz}\right] = \frac{4k_B T k_{eff}}{\omega_0 Q}$
© 2006

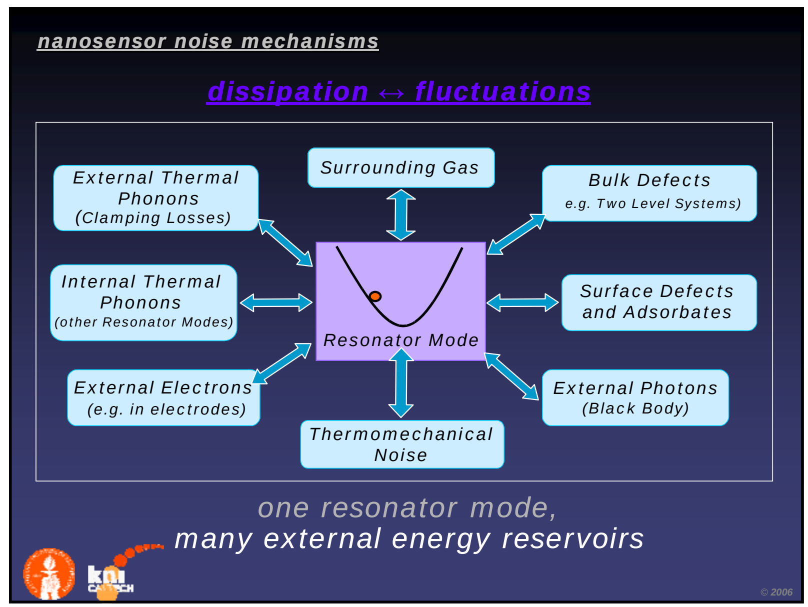
nanosensor noise mechanisms
dissipation ↔ fluctuations
External Thermal Phonons (Clamping Losses)
Surrounding Gas
Bulk Defects e.g. Two Level Systems)
Internal Thermal Phonons (other Resonator Modes)
Resonator Mode
Surface Defects and Adsorbates
External Electrons (e.g. in electrodes)
Thermomechanical Noise
External Photons (Black Body)
one resonator mode, many external energy reservoirs
© 2006

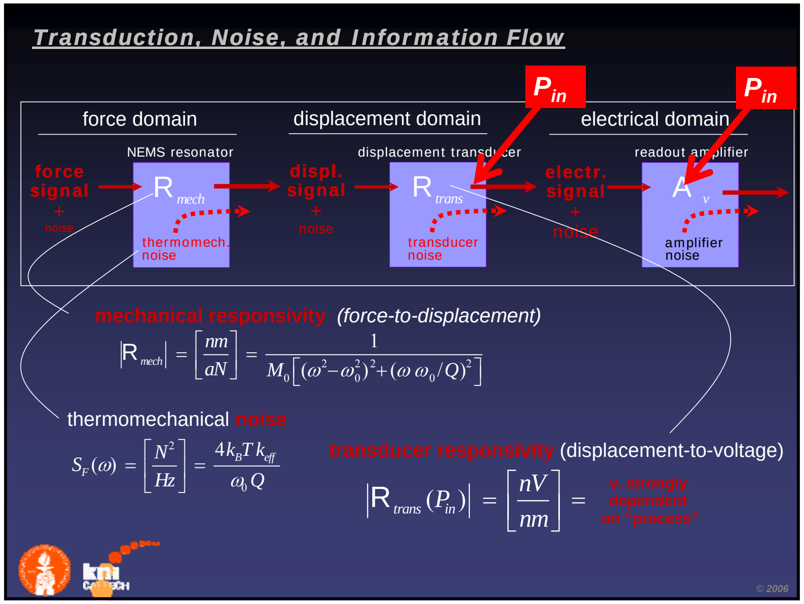
Transduction, Noise, and Information Flow
force domain
displacement domain
electrical domain
P_{in}
P_{in}
NEMS resonator
displacement transducer
readout amplifier
force signal + noise
R_{mech}
thermomech. noise
displ. signal + noise
R_{trans}
transducer noise
electr. signal + noise
A_v
amplifier noise
mechanical responsivity (force-to-displacement)
$|R_{mech}| = \left[\frac{nm}{aN}\right] = \frac{1}{M_0\left[(\omega^2-\omega_0^2)^2+(\omega\,\omega_0/Q)^2\right]}$
thermomechanical noise
$S_F(\omega) = \left[\frac{N^2}{Hz}\right] = \frac{4k_BTk_{eff}}{\omega_0 Q}$
transducer responsivity (displacement-to-voltage)
$|R_{trans}(P_{in})| = \left[\frac{nV}{nm}\right] =$ v. strongly dependent on "process"
© 2006

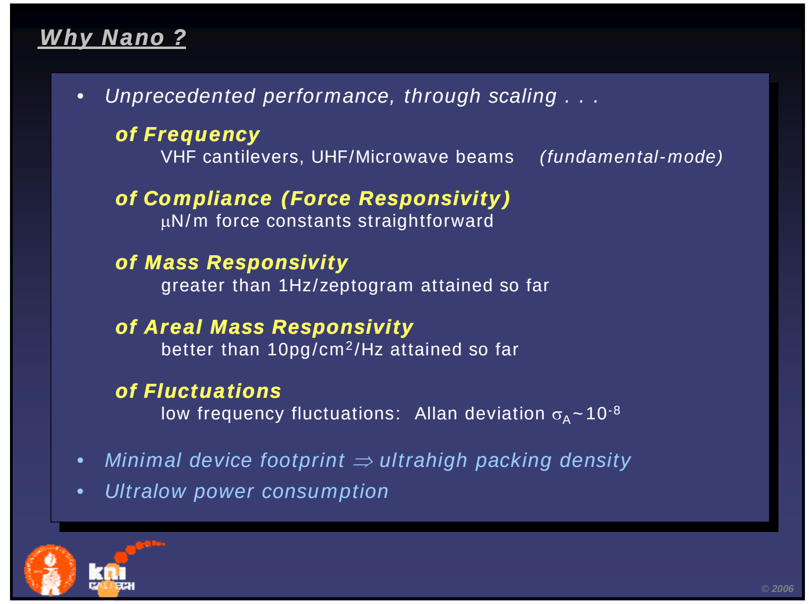
Why Nano ?
• Unprecedented performance, through scaling . . .
of Frequency
VHF cantilevers, UHF/Microwave beams (fundamental-mode)
of Compliance (Force Responsivity)
μN/m force constants straightforward
of Mass Responsivity
greater than 1Hz/zeptogram attained so far
of Areal Mass Responsivity
better than 10pg/cm²/Hz attained so far
of Fluctuations
low frequency fluctuations: Allan deviation $\sigma_A \sim 10^{-8}$
• Minimal device footprint ⇒ ultrahigh packing density
• Ultralow power consumption
© 2006

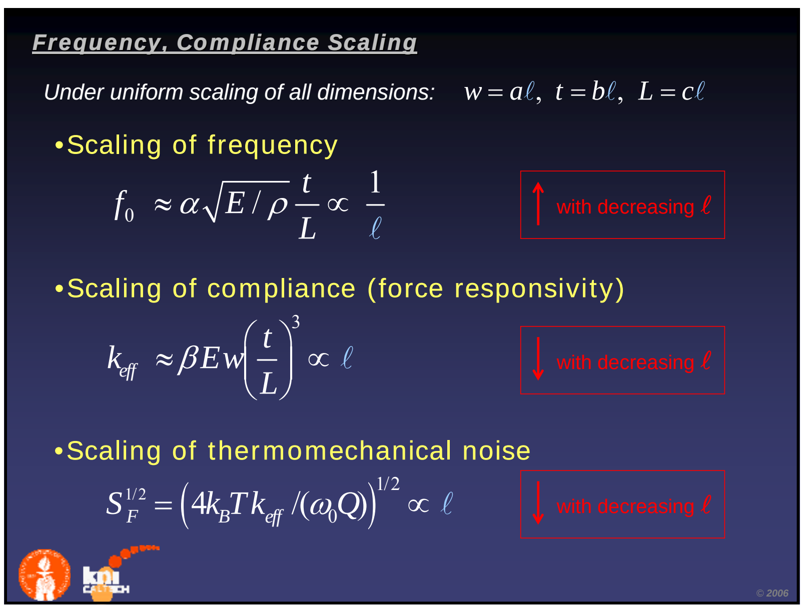
Frequency, Compliance Scaling
Under uniform scaling of all dimensions: $w = a\ell,\ t = b\ell,\ L = c\ell$
•Scaling of frequency
$f_0 \approx \alpha\sqrt{E/\rho}\,\frac{t}{L} \propto \frac{1}{\ell}$
↑ with decreasing ℓ
•Scaling of compliance (force responsivity)
$k_{eff} \approx \beta E w\left(\frac{t}{L}\right)^3 \propto \ell$
↓ with decreasing ℓ
•Scaling of thermomechanical noise
$S_F^{1/2} = \left(4k_BTk_{eff}/(\omega_0 Q)\right)^{1/2} \propto \ell$
↓ with decreasing ℓ
© 2006

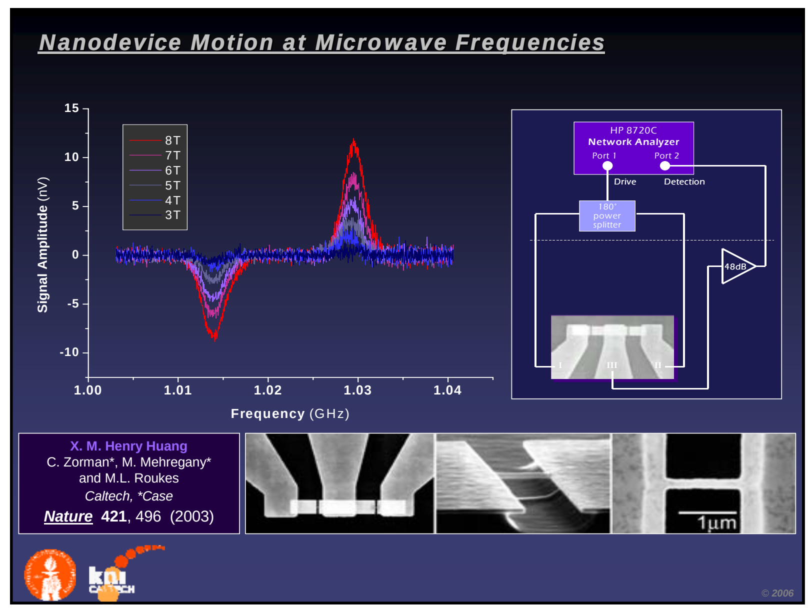
Nanodevice Motion at Microwave Frequencies
Signal Amplitude (nV)
Frequency (GHz)
8T
7T
6T
5T
4T
3T
HP 8720C Network Analyzer
Port 1
Port 2
Drive
Detection
180° power splitter
48dB
X. M. Henry Huang
C. Zorman*, M. Mehregany* and M.L. Roukes
Caltech, *Case
Nature 421, 496 (2003)
1μm
© 2006

Self-sensing Nanomechanical Force Sensors (2005-06)

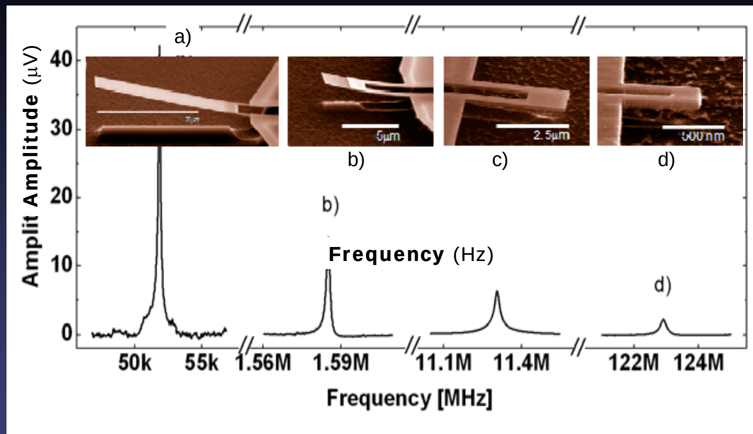

Noise Floor & Dynamic Range

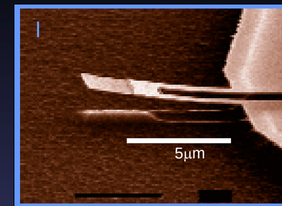

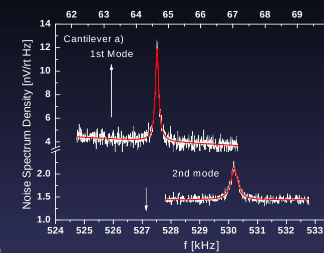

H.X. Tang, M. Li, M. Roukes, US patent pending
M. Li, H. Tang, M. Roukes, to be published (2006)

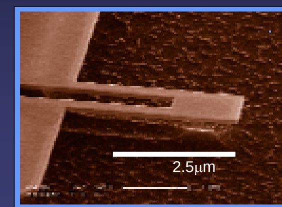

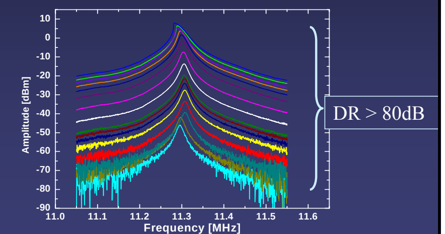

VHF/UHF NEMS Applications

- *Mass sensing*: **toward *1yg* resolution**
  – single-molecule mass spectrometry
- *Gas phase sensing*
  toward ultrafast ~ppt-concentration sensing
  at ambient temperature & pressure
- *Force sensing in vacuo*: **toward *100zN* resolution**
  next-gen scanning probe microscopy
  single-nucleus magnetic resonance imaging
- *Force sensing in fluid*: **toward *fN*-scale resolution**
  High BW / high sensitivity biological force sensing
- *Energy sensing*: **toward *μeV* resolution**
  measurements at the level of single mechanical quanta

Future proteomics

Toward single-molecule mass spectrometry

Roukes Group: **Dr. Wayne Hiebert** (NINT), **Selim Hanay, Dr. Philip Feng, Mo Li, Ben Gudlewski, Dr. Akshay Naik** *(11/1/06)*	**Caltech**
Prof. Kamil Ekinci	**Boston U.**
Prof. Milan Mrksich	**U. Chicago**
Prof. Stephen Quake	**Stanford U.**

mass spectrometry and proteomics

"At present there is no other technology visible that can rival the speed, sensitivity, and exact molecular characterization of MS methods of protein characterization".
Perspectives for Mass Spectrometry and Functional Proteomics, J. Godovac-Zimmermann, and L. R. Brown, *Mass Spectrometry Reviews*, **20**, 1-57 (2001).

"Realistically, we probably need (sensitivity) to be down to the level of about 10 copies per cell on the assumption that if you have 10 copies in a cell, they're actually doing something of note."
Brian T. Chait, Director, Mass Spectrometry and Gaseous Ion Chemistry Lab, Rockefeller University (2001)

"MS-based proteomics is still an emerging technology where revolutionary change is possible. ... Recent successes illustrate the role of mass spectrometry-based proteomics as an indispensable tool for molecular and cellular biology and for the emerging field of systems biology... The ability of mass spectrometry to identify and, increasingly, to precisely quantify thousands of proteins from complex samples can be expected to impact broadly on biology and medicine... "
Mass Spectrometry-Based Proteomics, Ruedi Aebersold and Matthias Mann, Nature **422**, 198-207 (2003).

mass spec: the state-of-the-art

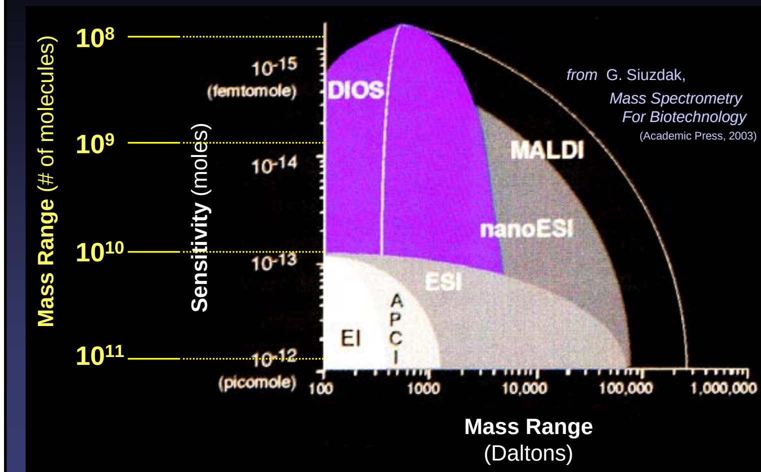

from G. Siuzdak, *Mass Spectrometry For Biotechnology* (Academic Press, 2003)

Inertial Mass Sensing

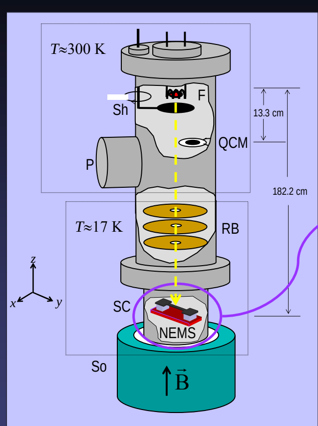

UHV microwave cryostat

two-port, HF NEMS resonator

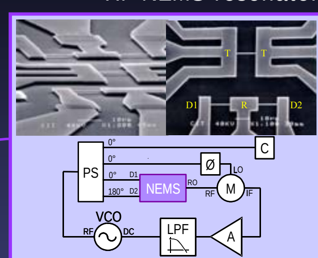

low noise, phase locked loop detection

Kamil Ekinci, Caltech '99

Mass Resolution: Ingredients

$$\delta M \approx \frac{\partial M_{eff}}{\partial \omega_0} \delta\omega_0 \sim R^{-1} \sigma_A(\tau)$$

mass resolution — R^{-1}: mass resp. — $\sigma_A(\tau)$: Allan deviation

large mass responsivity

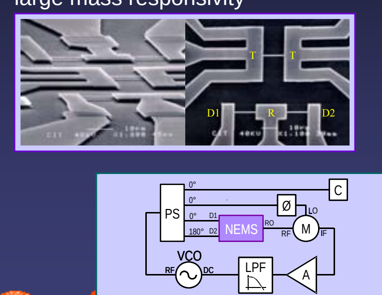

frequency resolution

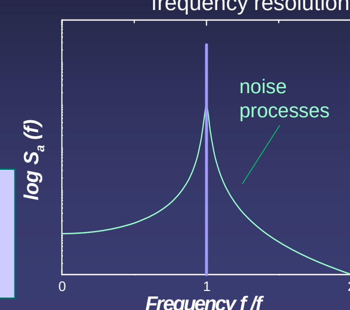

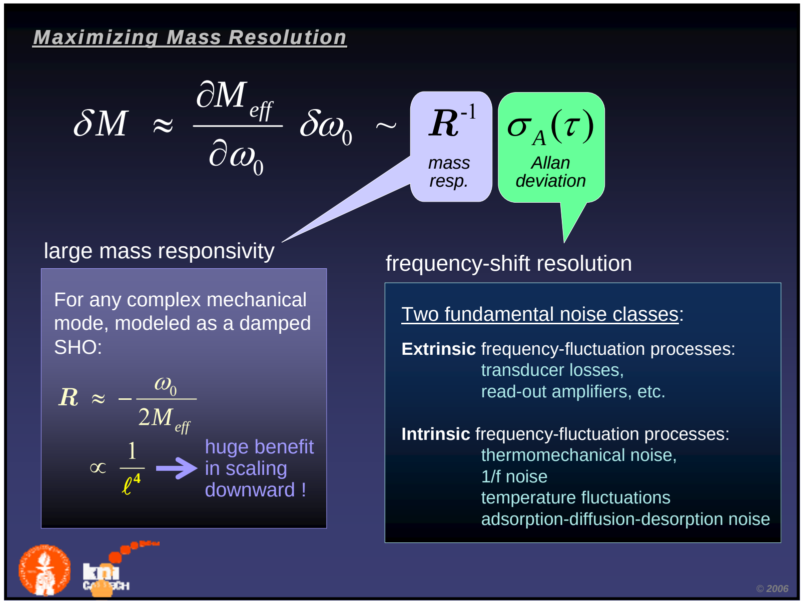
Maximizing Mass Resolution
$\delta M \approx \frac{\partial M_{eff}}{\partial \omega_0} \delta\omega_0 \sim R^{-1} \sigma_A(\tau)$
mass resp.
Allan deviation
large mass responsivity
For any complex mechanical mode, modeled as a damped SHO:
$R \approx -\frac{\omega_0}{2M_{eff}} \propto \frac{1}{\ell^4}$
huge benefit in scaling downward !
frequency-shift resolution
Two fundamental noise classes:
Extrinsic frequency-fluctuation processes:
transducer losses,
read-out amplifiers, etc.
Intrinsic frequency-fluctuation processes:
thermomechanical noise,
1/f noise
temperature fluctuations
adsorption-diffusion-desorption noise

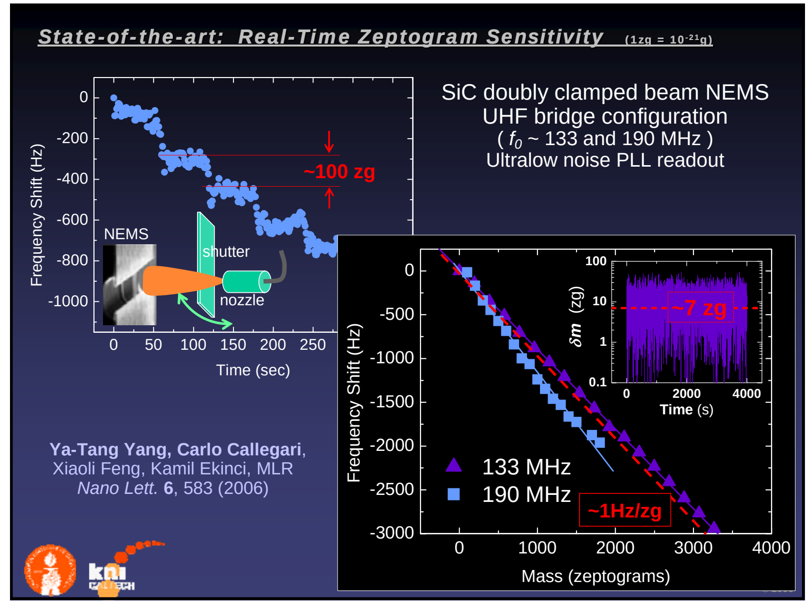
State-of-the-art: Real-Time Zeptogram Sensitivity (1zg = 10-21g)
SiC doubly clamped beam NEMS
UHF bridge configuration
(f_0 ~ 133 and 190 MHz)
Ultralow noise PLL readout
Frequency Shift (Hz)
Time (sec)
~100 zg
NEMS
shutter
nozzle
Ya-Tang Yang, Carlo Callegari,
Xiaoli Feng, Kamil Ekinci, MLR
Nano Lett. 6, 583 (2006)
δm (zg)
Time (s)
~7 zg
133 MHz
190 MHz
~1Hz/zg
Mass (zeptograms)

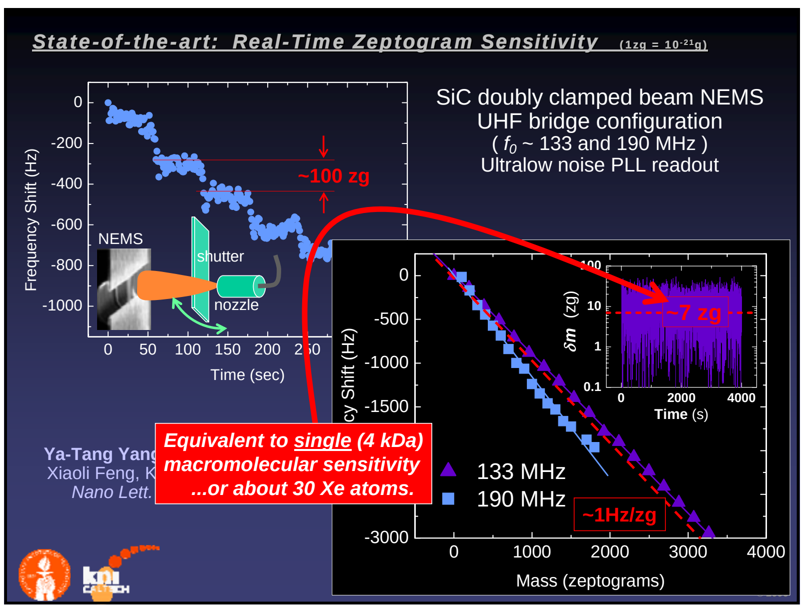
State-of-the-art: Real-Time Zeptogram Sensitivity (1zg = 10-21g)
SiC doubly clamped beam NEMS
UHF bridge configuration
(f_0 ~ 133 and 190 MHz)
Ultralow noise PLL readout
Frequency Shift (Hz)
Time (sec)
~100 zg
NEMS
shutter
nozzle
~7 zg
Time (s)
Equivalent to single (4 kDa) macromolecular sensitivity ...or about 30 Xe atoms.
133 MHz
190 MHz
~1Hz/zg
Mass (zeptograms)

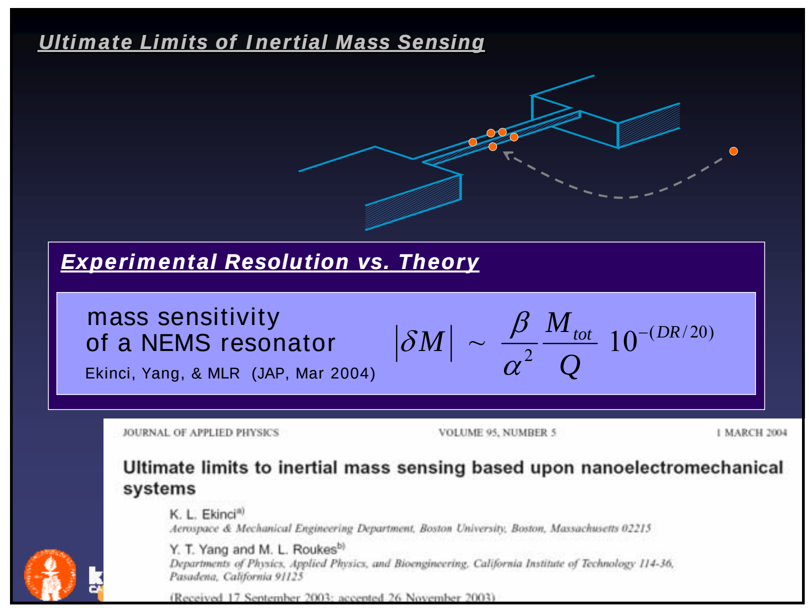
Ultimate Limits of Inertial Mass Sensing
Experimental Resolution vs. Theory
mass sensitivity
of a NEMS resonator
$|\delta M| \sim \frac{\beta}{\alpha^2}\frac{M_{tot}}{Q} 10^{-(DR/20)}$
Ekinci, Yang, & MLR (JAP, Mar 2004)
JOURNAL OF APPLIED PHYSICS VOLUME 95, NUMBER 5 1 MARCH 2004
Ultimate limits to inertial mass sensing based upon nanoelectromechanical systems
K. L. Ekinci
Aerospace & Mechanical Engineering Department, Boston University, Boston, Massachusetts 02215
Y. T. Yang and M. L. Roukes
Departments of Physics, Applied Physics, and Bioengineering, California Institute of Technology 114-36, Pasadena, California 91125
(Received 17 September 2003; accepted 26 November 2003)

toward next-gen NEMS mass responsivities

Achieved (top-down SiC NEMS), and **coupled** to low-noise PLL readout

f_0	NEMS Device Dimensions	Q	M_{eff}	DR	σ_A	δm
295 MHz	2.66μm × 170nm × 80nm	3000	118 fg	80 dB	4.7×10^{-8}	15 zg
420 MHz	1.8μm × 150nm × 100nm	1200	82 fg	90 dB	3.1×10^{-7}	67 zg
411 MHz	1.7μm × 120nm × 80nm	2600	53 fg	85 dB	6.6×10^{-8}	10 zg
428 MHz	1.65μm × 120nm × 80nm	2500	55 fg	90 dB	2.5×10^{-8}	4 zg
482 MHz	1.6μm × 120nm × 80nm	2000	52 fg	98 dB	2.1×10^{-8}	3 zg

1 kDa = 1.66 zg

Science **312**, 683 (5 May 2006)


NEWSFOCUS

PHYSICS

Tipping the Scales—Just Barely

Researchers are making big strides in a race to build nano-sized devices capable of weighing a single proton

Next to Kate Moss, Michael Roukes may be the most obsessive weight watcher on Earth. Roukes, a physicist at the California Institute of Technology (Caltech) in Pasadena, isn't particularly worried about putting on or shedding a kilogram. He's thinking much lighter than that. In the 4 April issue of *Nano Letters*, Roukes and colleagues report making the most sensitive mechanical scale ever, capable of registering 0.000000000000000000007 grams, or 7 zeptograms.

mass slowed the bridge's vibrations, causing a change in the pattern of voltage readouts.

Ekinci says that since 2002 the team has improved the sensitivity of its apparatus 1000-fold. But he says it will take another such jump to detect individual hydrogen atoms. "This approach has very good potential to go to higher sensitivity," Ekinci says. To succeed, however, Ekinci and Roukes will need to make slightly smaller, more responsive bridges, get them to oscillate at a slightly higher frequency, and tweak the feedback circuitry to improve detection. Each advance has already been demonstrated independently; now Roukes's current team is working on putting them all together.

Other groups are also hard at work. One, led by Andrew Cleland at the University of California, Santa Barbara, for example, is using thermal

Why 1 yg?

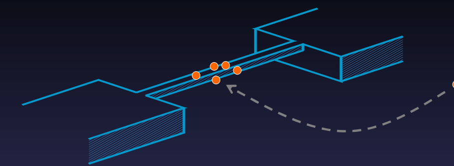

Toward Single-Dalton Resolution

- **Next-generation NEMS resonators is a ~0.85 GHz resonator** (with M_{tot}~2×10^{-16} g). **Expected advances should yield Q~10^4 and DR~80dB at this frequency, to yield a resolution δM ~1.6 × 10^{-24} g , i.e. 1Da.**
- **This will yield *atomic resolution*, with sufficient sensitivity to detect a single adsorbed hydrogen atom.**
- **N.B.: *(a)* the species need not be charged to be detected.**
  ***(b)* no mass preselection is required (each molecule is *weighed*)**

Current Efforts: *real-time, electrospray injection to NEMS*

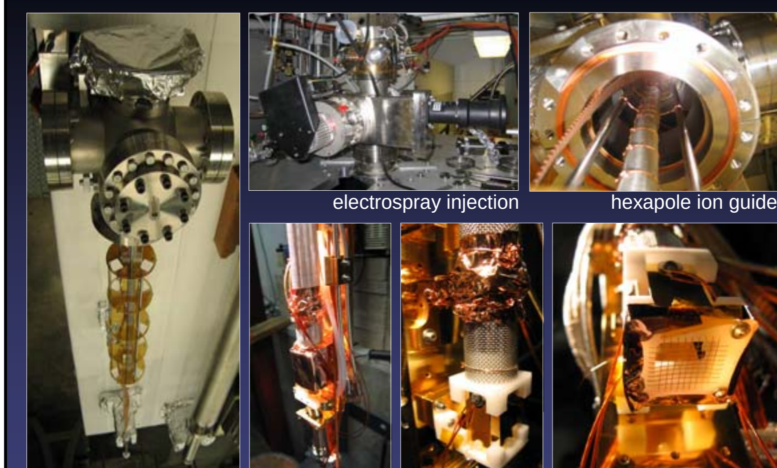

electrospray injection

hexapole ion guide

Wayne Hiebert, Selim Hanay, Steve Stryker, MLR (*2004-06*)

Microfluidics + Nanoelectrospray

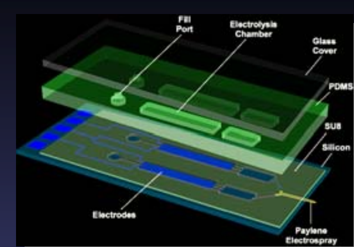

Chip-based separation plus nanoelectrospray injection

(Tai Group, *Caltech*)

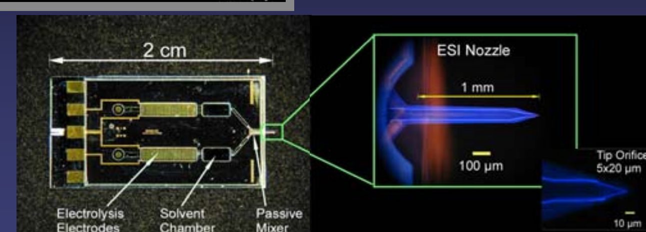

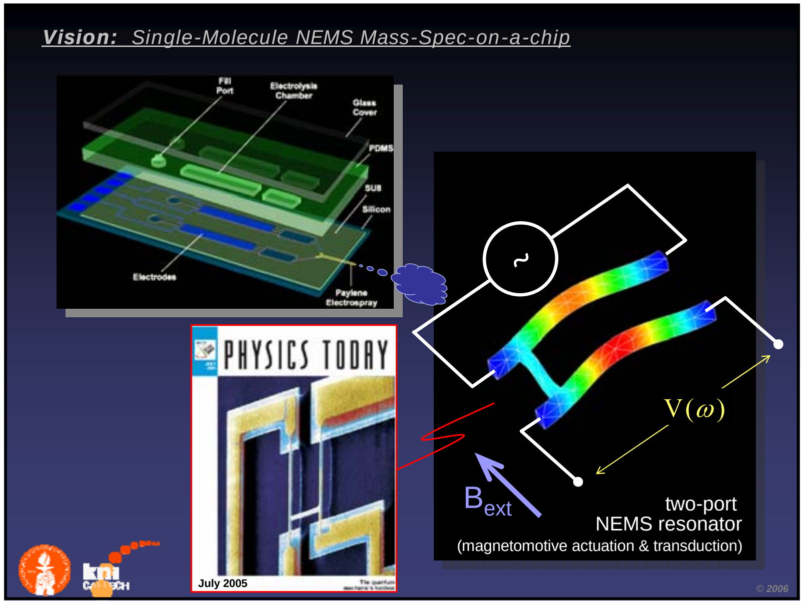
Vision: Single-Molecule NEMS Mass-Spec-on-a-chip
Fill Port
Electrolysis Chamber
Glass Cover
PDMS
SU8
Silicon
Electrodes
Paylene Electrospray
PHYSICS TODAY
July 2005
V(ω)
B ext
two-port
NEMS resonator
(magnetomotive actuation & transduction)
© 2006

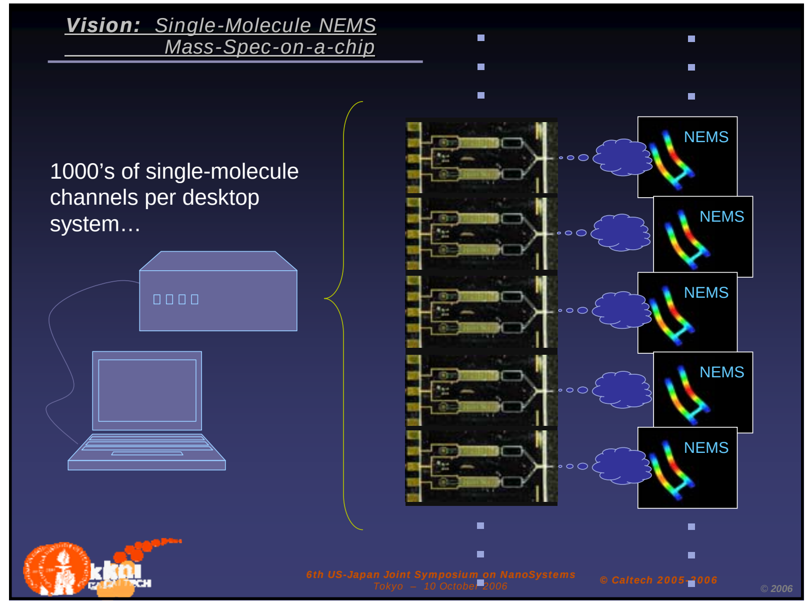
Vision: Single-Molecule NEMS Mass-Spec-on-a-chip
1000's of single-molecule channels per desktop system…
NEMS
NEMS
NEMS
NEMS
NEMS
6th US-Japan Joint Symposium on NanoSystems
© Caltech 2005-2006
© 2006


Nanoelectromechanical "Nose"
Toward early-stage disease diagnosis via breath analysis
Roukes Group:
Dr. Ed Myers, Dr. Sequoyah Aldridge,
Dr. Philip Feng, Mo Li, Ben Gudlewski
Lewis Group:
Prof. Nathan Lewis, Heather McCaig
Caltech
Dr. R.J. (Joe) Simonson
Dr. Josh Whiting
Dr. David Wheeler
Dr. Shawn Dirk
Sandia
Prof. Hong Tang
Yale U.
© 2006

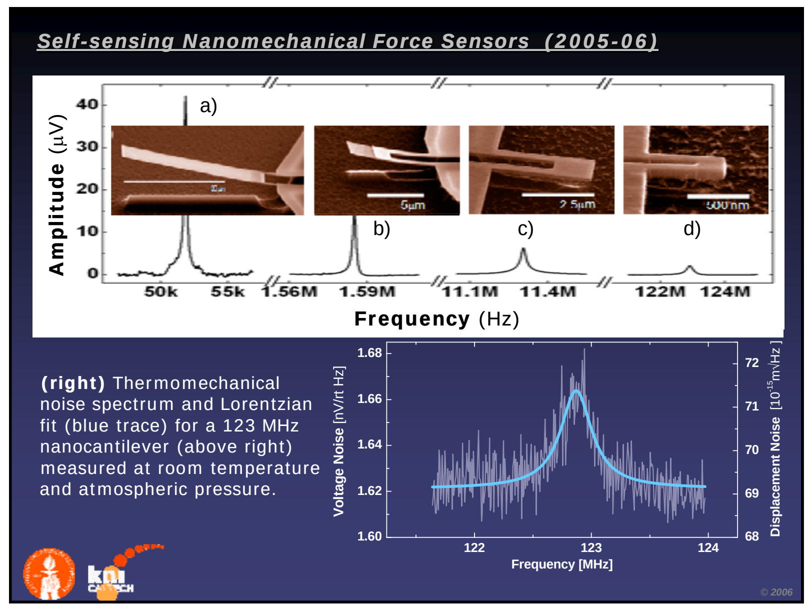
Self-sensing Nanomechanical Force Sensors (2005-06)
Amplitude (μV)
40
30
20
10
0
a)
b)
c)
d)
50k
55k
1.56M
1.59M
11.1M
11.4M
122M
124M
Frequency (Hz)
(right) Thermomechanical noise spectrum and Lorentzian fit (blue trace) for a 123 MHz nanocantilever (above right) measured at room temperature and atmospheric pressure.
Voltage Noise [nV/rt Hz]
1.68
1.66
1.64
1.62
1.60
122
123
124
Frequency [MHz]
72
71
70
69
68
Displacement Noise
© 2006

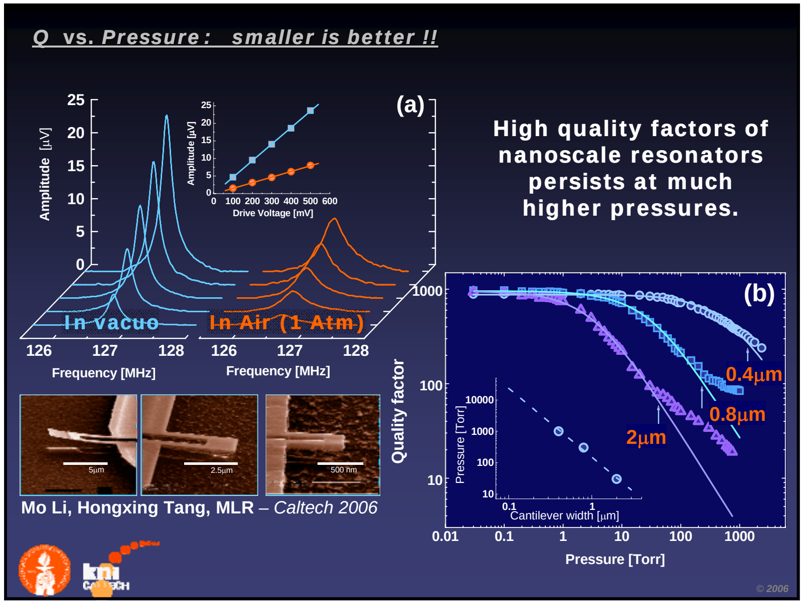
Q vs. Pressure: smaller is better !!
(a)
High quality factors of nanoscale resonators persists at much higher pressures.
Amplitude [µV]
Drive Voltage [mV]
In vacuo
In Air (1 Atm)
Frequency [MHz]
(b)
Quality factor
0.4µm
0.8µm
2µm
Pressure [Torr]
Cantilever width [µm]
Mo Li, Hongxing Tang, MLR – Caltech 2006
© 2006

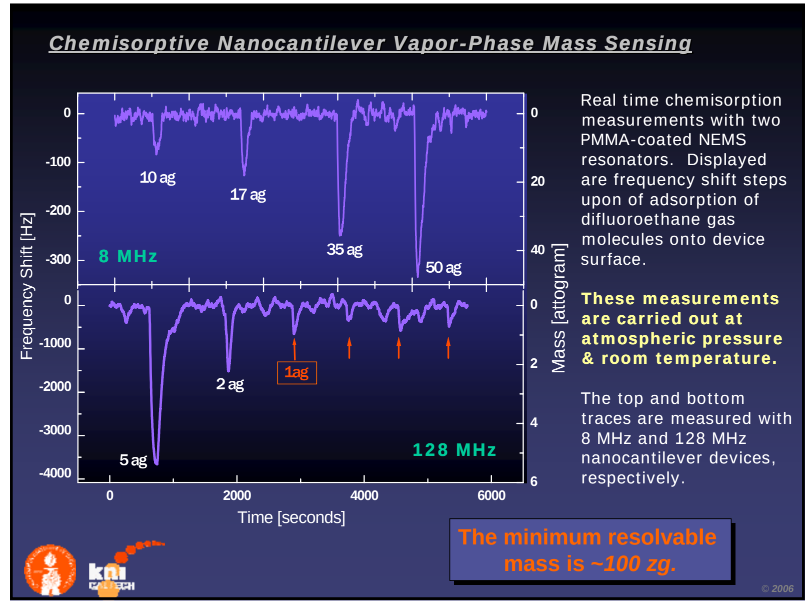
Chemisorptive Nanocantilever Vapor-Phase Mass Sensing
Frequency Shift [Hz]
Mass [attogram]
Time [seconds]
8 MHz
10 ag
17 ag
35 ag
50 ag
128 MHz
5 ag
2 ag
1ag
Real time chemisorption measurements with two PMMA-coated NEMS resonators. Displayed are frequency shift steps upon of adsorption of difluoroethane gas molecules onto device surface.
These measurements are carried out at atmospheric pressure & room temperature.
The top and bottom traces are measured with 8 MHz and 128 MHz nanocantilever devices, respectively.
The minimum resolvable mass is ~100 zg.
© 2006

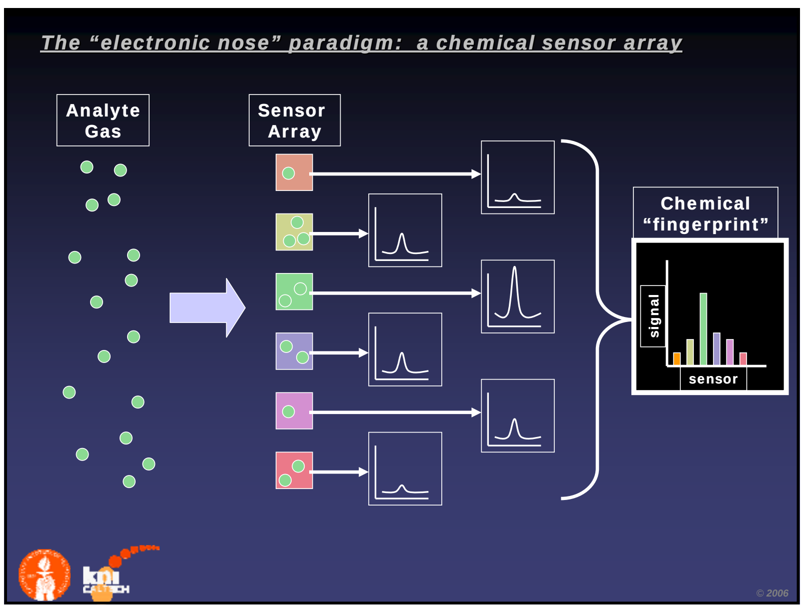
The “electronic nose” paradigm: a chemical sensor array
Analyte Gas
Sensor Array
Chemical “fingerprint”
signal
sensor
© 2006

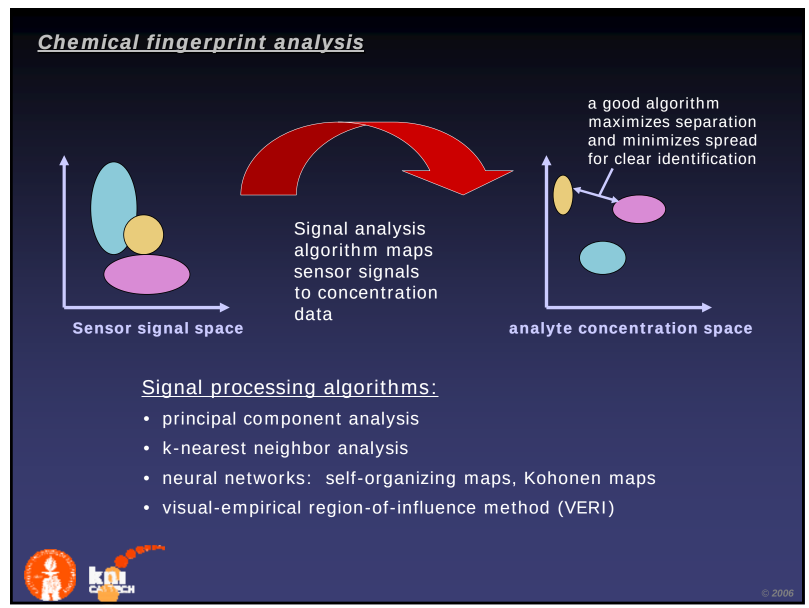
Chemical fingerprint analysis
Sensor signal space
Signal analysis algorithm maps sensor signals to concentration data
a good algorithm maximizes separation and minimizes spread for clear identification
analyte concentration space
Signal processing algorithms:
• principal component analysis
• k-nearest neighbor analysis
• neural networks: self-organizing maps, Kohonen maps
• visual-empirical region-of-influence method (VERI)
© 2006

Electromechanical nose for clinical medicine?

Four independent studies have recently shown that vapor-phase screening technology can reveal volatile organic compounds (VOCs) on patients' breath that are biomarkers for lung cancer.
For lung cancer, as well as for other diseases, specific VOCs can thus be correlated with, and are indicative of, disease conditions not present in healthy patient controls.

Table 1. Summary of the main volatile organic compounds (VOCs) associated with different disease types, as analyzed as chromatography (GC) or GC-linked with mass spectrometry (GC-MS).

Disorder	VOC source	VOC Target
Urinary tract infection	urine	isovaleric acid, alkanes
Aerobic gram-negative bacteria	intra-peritoneal fluid	terpenes, ketones
Anaerobic bacterial infections	intra-peritoneal fluid	acetic, butyric acid
Bacterial vaginosis	vaginal cavity and discharge	amines
Breast cancer	human breath, lung air	2,3-dimethyl-pentane, 2-methyl-pentane, 3-methyl-pentane
Lung cancer	human breath, lung air	alkanes, mono-methylated alkanes, aniline, o-toluidine
Acute asthma	human breath	pentane
Metabolic disorders	urine	isovaleric acid
Hepatic coma	alveolar air	methyl-mercaptan
Rheumatoid arthritis	alveolar air	pentane
Schizophrenia	alveolar air	pentane, carbon disulphide
Ketosis	alveolar air	acetone
Cardiopulmonary disease	alveolar air	acetone, ethanol
Hepatic encephalopathy	blood plasma, cerebrospinal fluid	3-methylbutanol
Uremia	breath, urine	dimethylamine, trimethylamine
Trimethylaminuria	breath, urine, sweat, vaginal discharge	trimethylamine
Diabetes mellitus	lung air, urine	acetone
Larynx cancer	breath	C_2 to C_8 aliphatic acids
Dysgeusia/Dysosmia	lung air	hydrogen sulfide, methyl mercaptan, pyridine, aniline, diphenylamine, dodecanol
Cystinuria	breath	cadaverine, piperidine, putrescine, pyrrolidine
Cirrhosis	breath	acetic acid, propionic acid, isobutyric acid, butyric acid, isovaleric acid, carbon disulphide
Histidinemia	breath	2-imidazolepyruvic acid, 2-imidazoleacetic acid, 2-imidazolelactic acid
Tyrosinemia	breath	p-hydroxyphenylpyruvic acid
Phenylketonuria	breath	phenylpyruvic acid, phenyllactic acid, phenylacetic acid
Maple syrup urine disease	breath	2-oxoisocaproic acid
Halitosis	mouth air	hydrogen sulfide, methyl mercaptan, cadaverine, putrescine, indole, skatole
Vaginal tumor	vaginal cavity	C_2 to C_8 aliphatic acids

VOCs in human breath

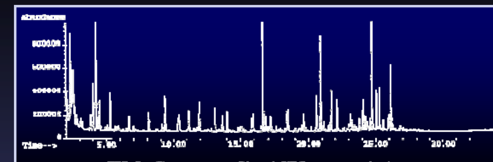

FIG. 1. Chromatogram of breath VOCs in a normal subject.

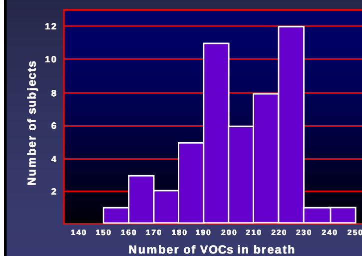

Recent study: (50 individuals)
- Approximately 3500 unique VOCs found; **~200 per person**
- **27 common VOCs**—almost all are alkanes or methylated alkanes

Origin of common VOCs:
- **Reactive oxygen species** are byproducts of normal metabolic processes
- These species then oxidize cellular material
- Normal oxidation thought to be important in aging process (**antioxidants** supposedly counteract this behavior)

- Byproduct of oxygen breakdown of cells is most often **alkanes,** which are then released into breath

Array signal processing yields biomarker identification

- Processing algorithms of sensor array response (e.g., principal component analysis) maps data into "analyte identification space".
- **Severin, Lewis *et al.*:**
  - An array of 20 chemiresistor sensors were used to resolve a generic, homologous series of VOCs, into **individual species and binary mixtures**.
  - Individual analytes can be distinguished using principal component analysis (PCA).

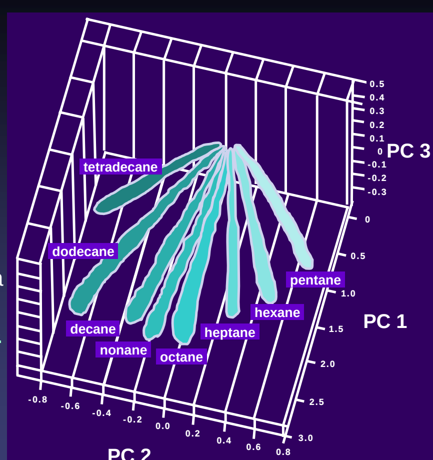

Severin, Lewis *et al.*, 2000

Caltech-Sandia Project: μGC + NEMS Sensor

***NEMS Nose*:**

A new paradigm based on microfluidic sample preconditioning and multiplexed arrays of ultrasensitive NEMS mass detectors (differentially functionalized)

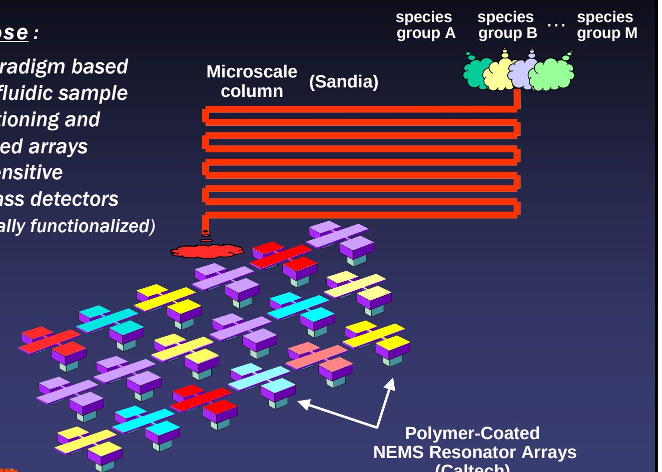

18

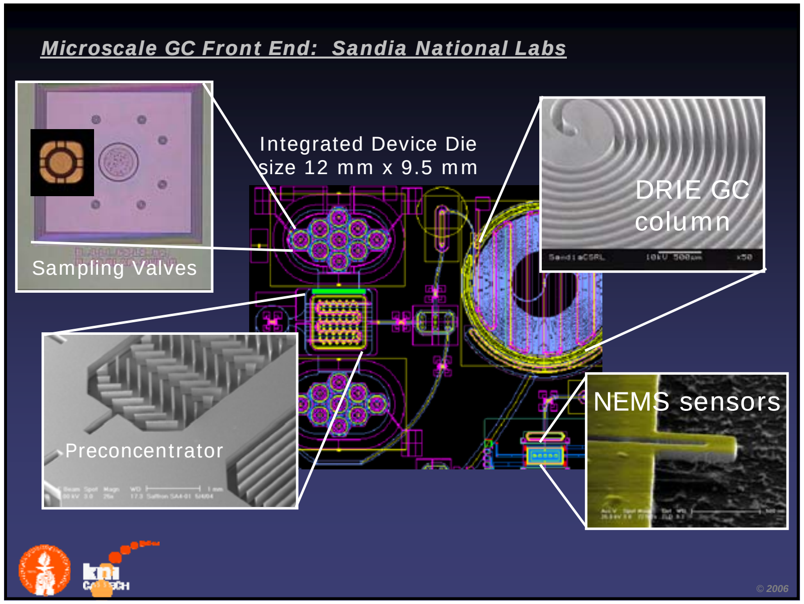
Microscale GC Front End: Sandia National Labs
Integrated Device Die
size 12 mm x 9.5 mm
DRIE GC column
Sampling Valves
Preconcentrator
NEMS sensors
© 2006

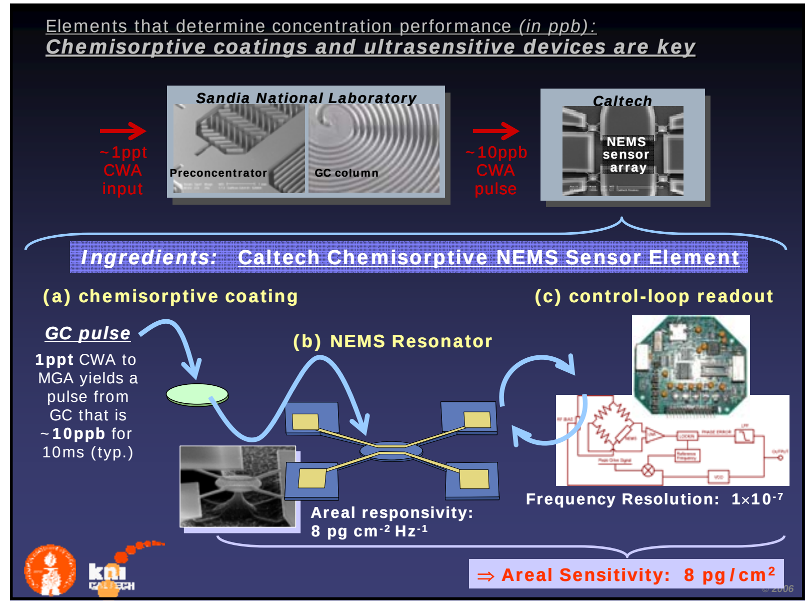
Elements that determine concentration performance (in ppb):
Chemisorptive coatings and ultrasensitive devices are key
~1ppt CWA input
Sandia National Laboratory
Preconcentrator
GC column
~10ppb CWA pulse
Caltech
NEMS sensor array
Ingredients: Caltech Chemisorptive NEMS Sensor Element
(a) chemisorptive coating
(c) control-loop readout
GC pulse
1ppt CWA to MGA yields a pulse from GC that is ~10ppb for 10ms (typ.)
(b) NEMS Resonator
Areal responsivity:
8 pg cm⁻² Hz⁻¹
Frequency Resolution: 1×10⁻⁷
⇒ Areal Sensitivity: 8 pg/cm²

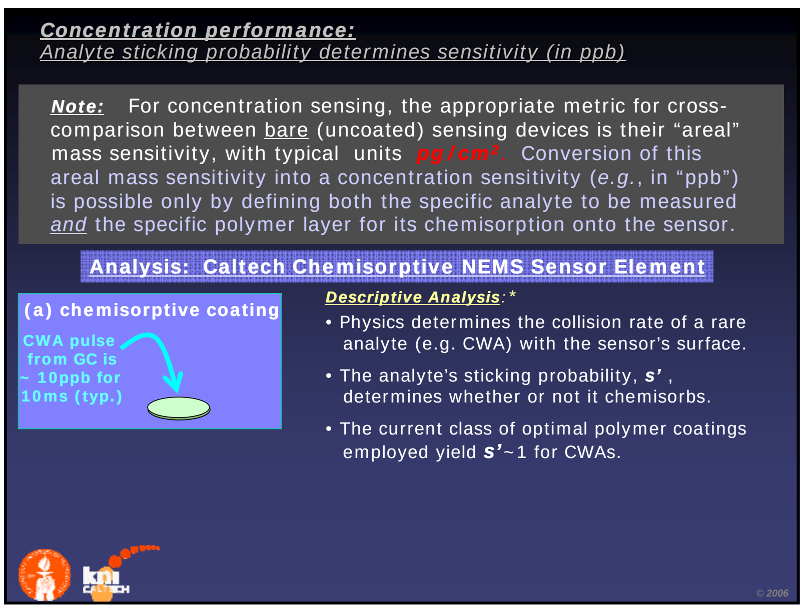
Concentration performance:
Analyte sticking probability determines sensitivity (in ppb)
Note: For concentration sensing, the appropriate metric for cross-comparison between bare (uncoated) sensing devices is their "areal" mass sensitivity, with typical units pg/cm². Conversion of this areal mass sensitivity into a concentration sensitivity (e.g., in "ppb") is possible only by defining both the specific analyte to be measured and the specific polymer layer for its chemisorption onto the sensor.
Analysis: Caltech Chemisorptive NEMS Sensor Element
(a) chemisorptive coating
CWA pulse from GC is ~ 10ppb for 10ms (typ.)
Descriptive Analysis:*
• Physics determines the collision rate of a rare analyte (e.g. CWA) with the sensor's surface.
• The analyte's sticking probability, s', determines whether or not it chemisorbs.
• The current class of optimal polymer coatings employed yield s'~1 for CWAs.
© 2006

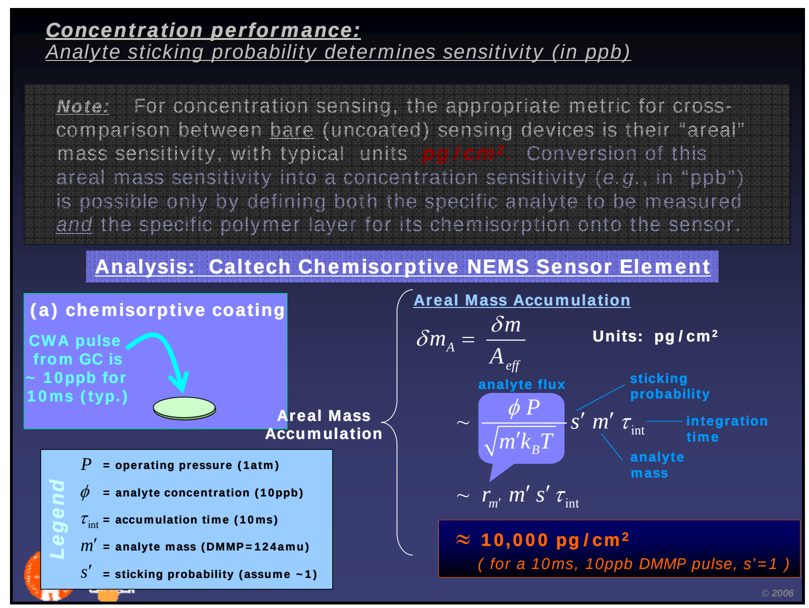
Concentration performance:
Analyte sticking probability determines sensitivity (in ppb)
Note: For concentration sensing, the appropriate metric for cross-comparison between bare (uncoated) sensing devices is their "areal" mass sensitivity, with typical units pg/cm². Conversion of this areal mass sensitivity into a concentration sensitivity (e.g., in "ppb") is possible only by defining both the specific analyte to be measured and the specific polymer layer for its chemisorption onto the sensor.
Analysis: Caltech Chemisorptive NEMS Sensor Element
(a) chemisorptive coating
CWA pulse from GC is ~ 10ppb for 10ms (typ.)
Areal Mass Accumulation
Areal Mass Accumulation
$\delta m_A = \frac{\delta m}{A_{eff}}$
Units: pg/cm²
analyte flux
sticking probability
$\sim \frac{\phi P}{\sqrt{m' k_B T}} s' m' \tau_{int}$
integration time
analyte mass
$\sim r_{m'} m' s' \tau_{int}$
Legend
P = operating pressure (1atm)
ϕ = analyte concentration (10ppb)
τ_{int} = accumulation time (10ms)
m' = analyte mass (DMMP=124amu)
s' = sticking probability (assume ~1)
≈ 10,000 pg/cm²
(for a 10ms, 10ppb DMMP pulse, s'=1)
© 2006

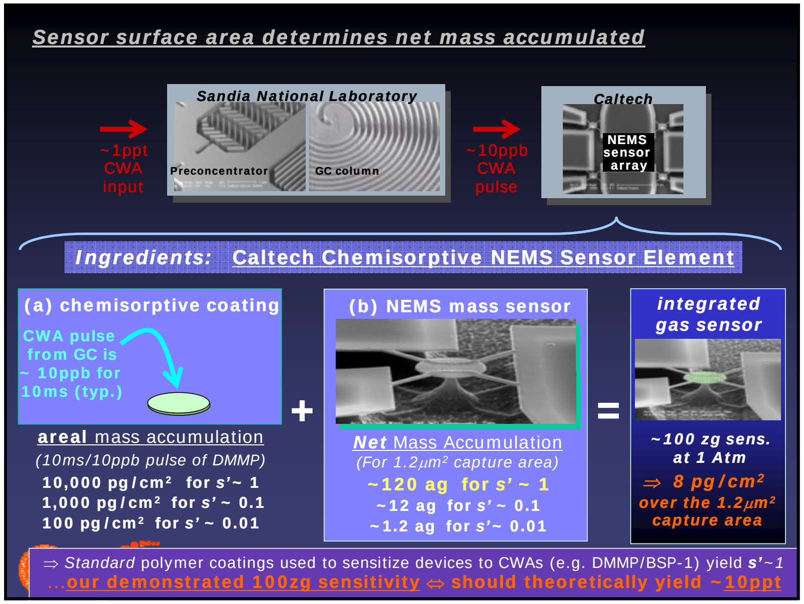

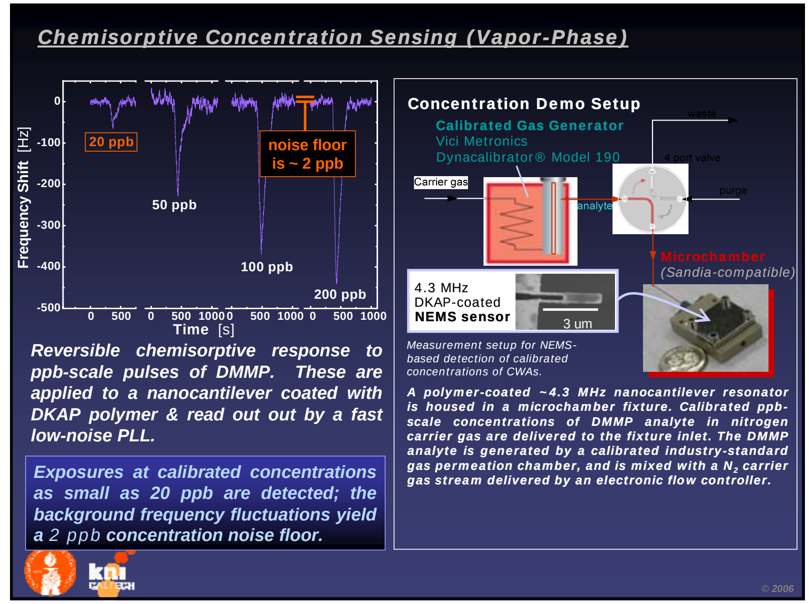

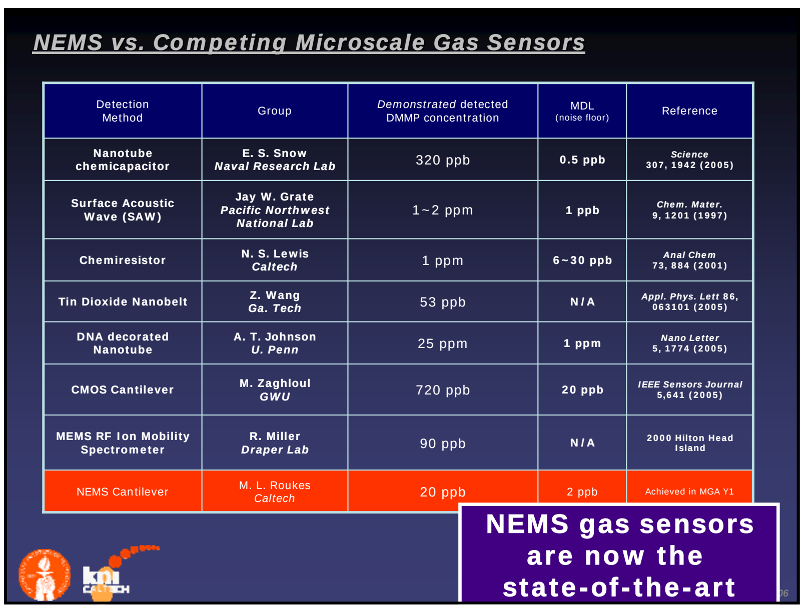

Detection Method	Group	*Demonstrated* detected DMMP concentration	MDL (noise floor)	Reference
Nanotube chemicapacitor	E. S. Snow *Naval Research Lab*	320 ppb	0.5 ppb	*Science* 307, 1942 (2005)
Surface Acoustic Wave (SAW)	Jay W. Grate *Pacific Northwest National Lab*	1~2 ppm	1 ppb	*Chem. Mater.* 9, 1201 (1997)
Chemiresistor	N. S. Lewis *Caltech*	1 ppm	6~30 ppb	*Anal Chem* 73, 884 (2001)
Tin Dioxide Nanobelt	Z. Wang *Ga. Tech*	53 ppb	N/A	*Appl. Phys. Lett* 86, 063101 (2005)
DNA decorated Nanotube	A. T. Johnson *U. Penn*	25 ppm	1 ppm	*Nano Letter* 5, 1774 (2005)
CMOS Cantilever	M. Zaghloul *GWU*	720 ppb	20 ppb	*IEEE Sensors Journal* 5,641 (2005)
MEMS RF Ion Mobility Spectrometer	R. Miller *Draper Lab*	90 ppb	N/A	2000 Hilton Head Island
NEMS Cantilever	M. L. Roukes *Caltech*	20 ppb	2 ppb	Achieved in MGA Y1

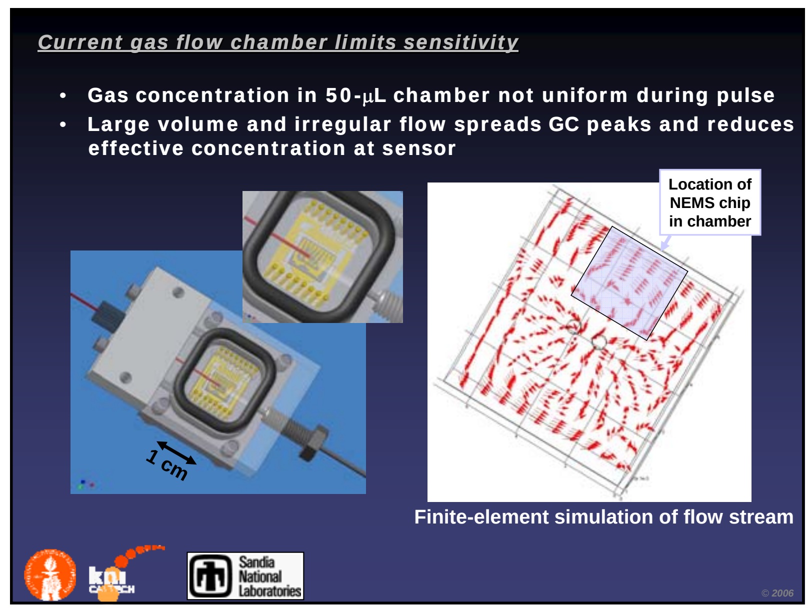

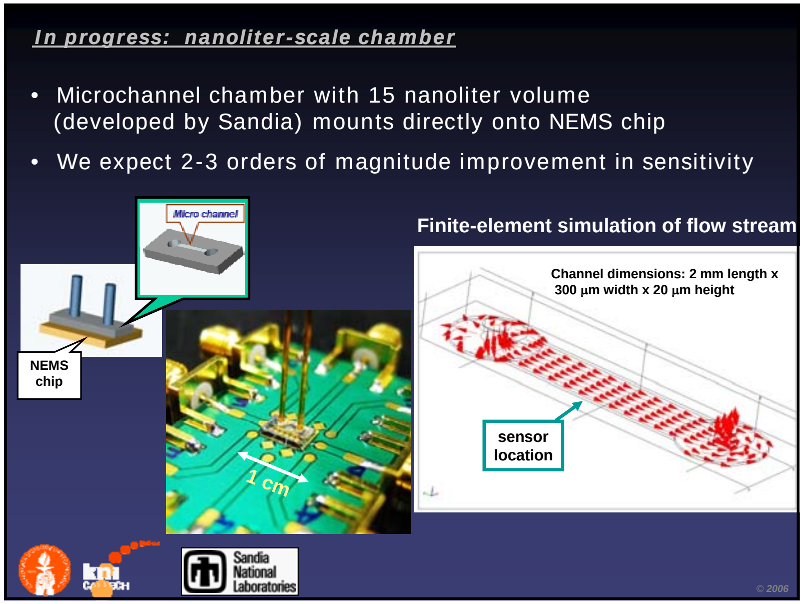
In progress: nanoliter-scale chamber
• Microchannel chamber with 15 nanoliter volume (developed by Sandia) mounts directly onto NEMS chip
• We expect 2-3 orders of magnitude improvement in sensitivity
Micro channel
NEMS chip
1 cm
Finite-element simulation of flow stream
Channel dimensions: 2 mm length x 300 μm width x 20 μm height
sensor location
Sandia National Laboratories
© 2006

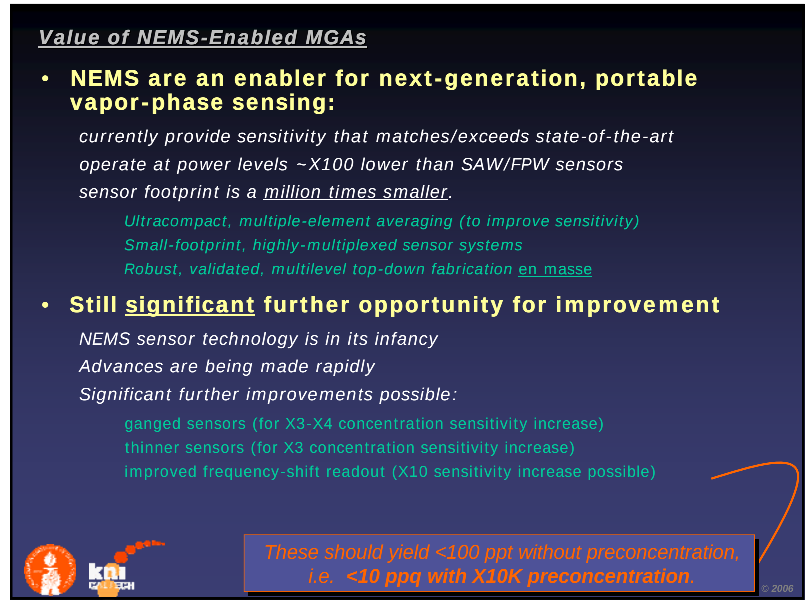
Value of NEMS-Enabled MGAs
• NEMS are an enabler for next-generation, portable vapor-phase sensing:
currently provide sensitivity that matches/exceeds state-of-the-art
operate at power levels ~X100 lower than SAW/FPW sensors
sensor footprint is a million times smaller.
Ultracompact, multiple-element averaging (to improve sensitivity)
Small-footprint, highly-multiplexed sensor systems
Robust, validated, multilevel top-down fabrication en masse
• Still significant further opportunity for improvement
NEMS sensor technology is in its infancy
Advances are being made rapidly
Significant further improvements possible:
ganged sensors (for X3-X4 concentration sensitivity increase)
thinner sensors (for X3 concentration sensitivity increase)
improved frequency-shift readout (X10 sensitivity increase possible)
These should yield <100 ppt without preconcentration, i.e. <10 ppq with X10K preconcentration.
© 2006

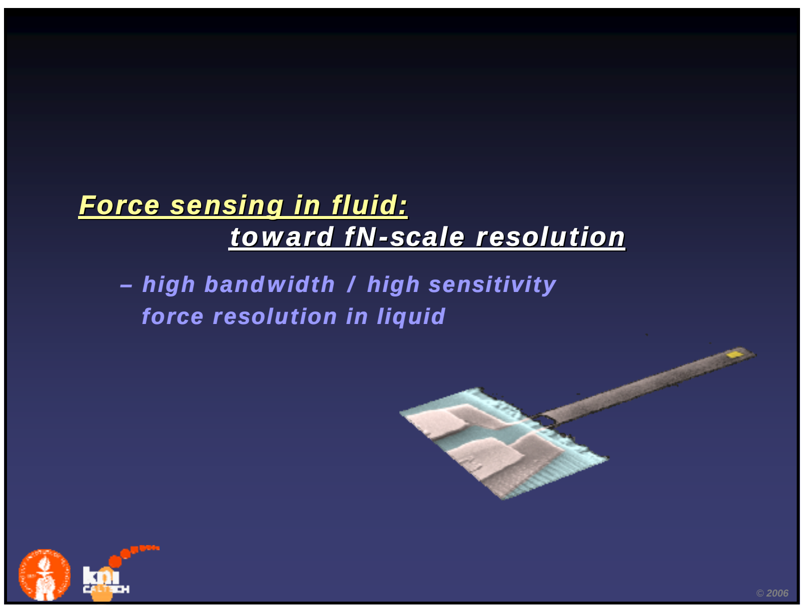
Force sensing in fluid:
toward fN-scale resolution
– high bandwidth / high sensitivity force resolution in liquid
© 2006

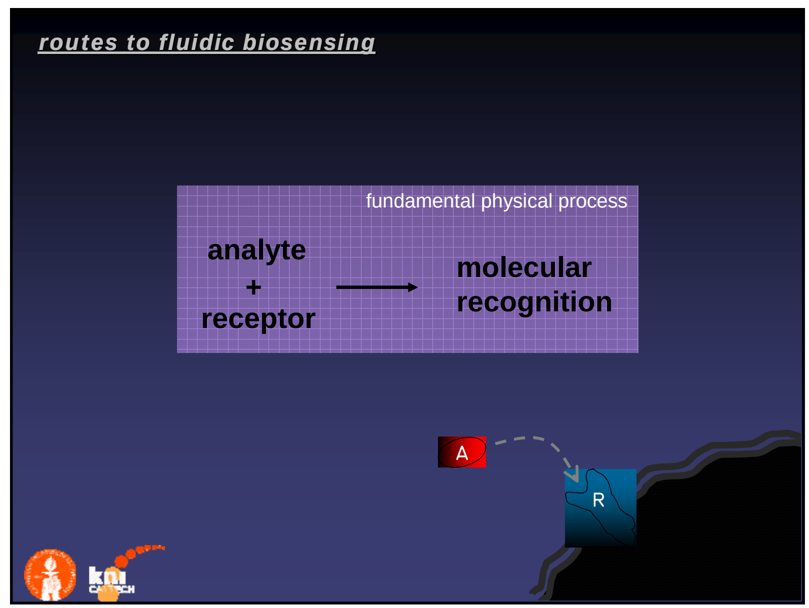
routes to fluidic biosensing
fundamental physical process
analyte + receptor
molecular recognition
A
R

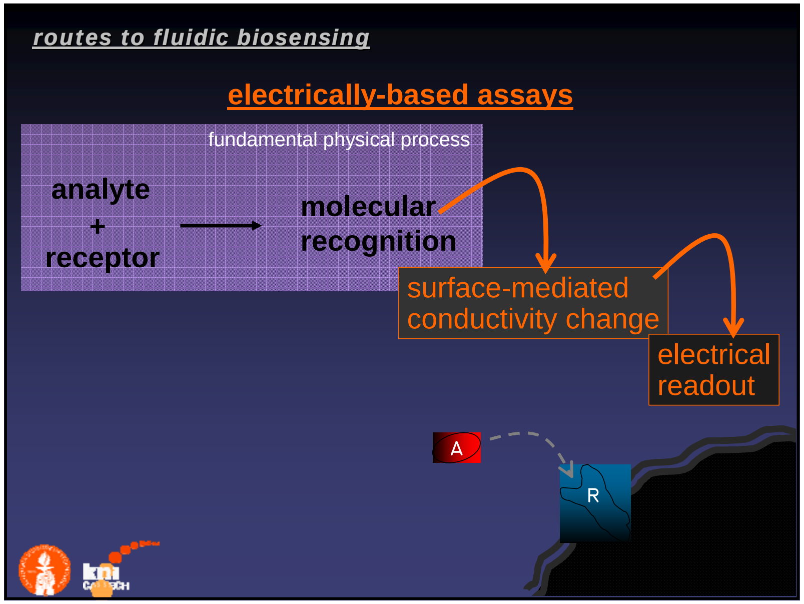

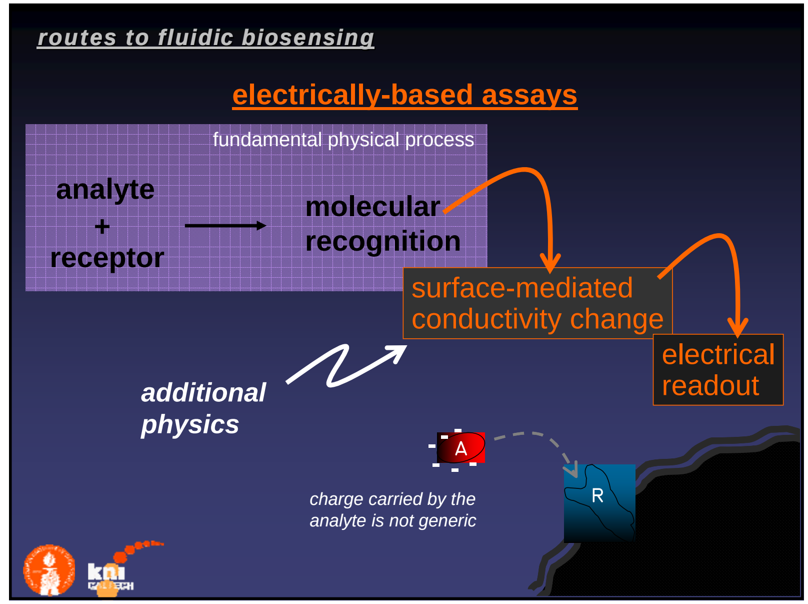

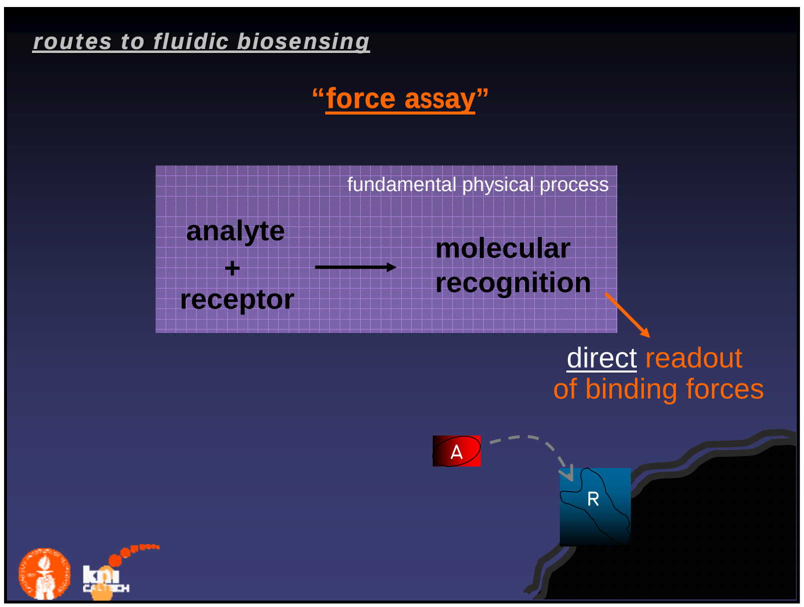

BioNEMS inspiration: single-molecule biophysics

Optical Tweezers
e.g. Chu, Block, Bustamante, …

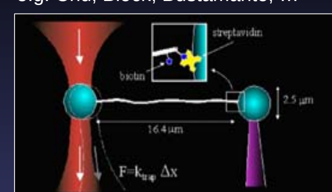

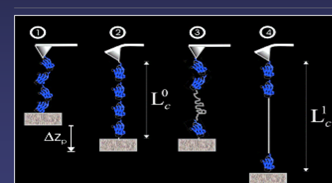

AFM-based (Force Spectroscopy)
e.g. Hansma, Gaub, Fernandez, …

Nature of Interaction	Interaction Force
Receptor/Ligand Interaction	**50–250pN**
Avidin-Biotin	**90–260 pN**
Antibody-Antigen	**50–300pN**
Cadherin-Cadherin	**35–55pN**
DNA Hybridization	**65pN–1.5nN**
Chemical Bond	**1–10nN**
Covalent(C-C, C-O, C-N)	**4.0–4.5nN**
Covalent (Au-S, Si-C)	**1–3nN**
H-bond	**10pN**
Unfolding Forces	**100–300pN**
Protein (Titin) unfolding	**150–300pN**
Dextran bond twists	**100–300pN**

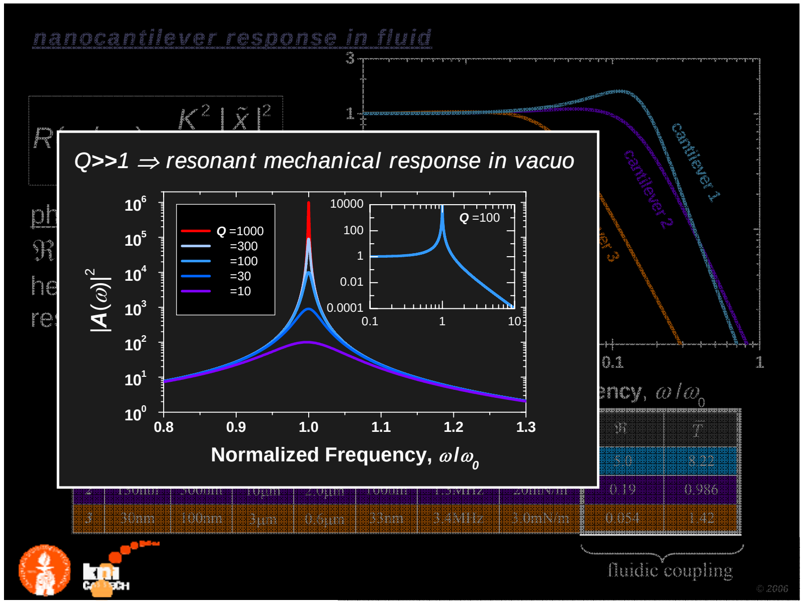

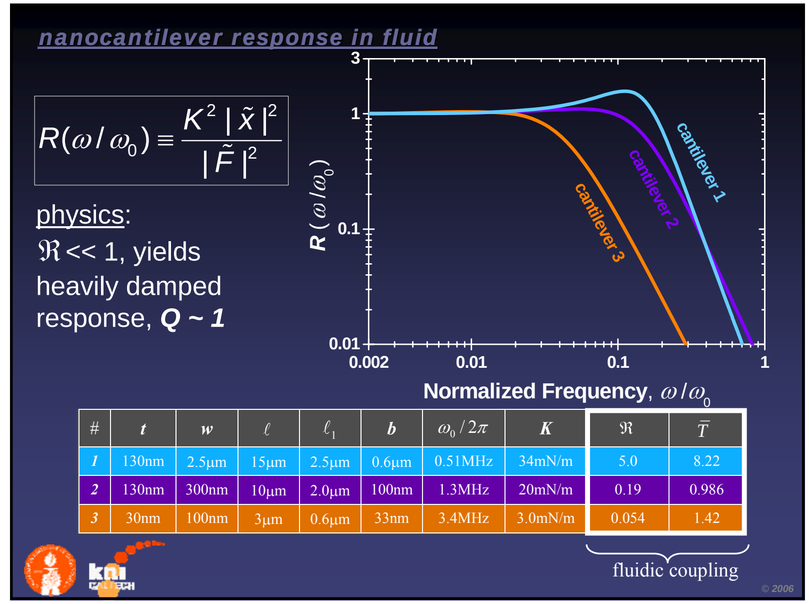

#	t	w	ℓ	ℓ_1	b	$\omega_0/2\pi$	K	$\Re$	$\bar{T}$
1	130nm	2.5µm	15µm	2.5µm	0.6µm	0.51MHz	34mN/m	5.0	8.22
2	130nm	300nm	10µm	2.0µm	100nm	1.3MHz	20mN/m	0.19	0.986
3	30nm	100nm	3µm	0.6µm	33nm	3.4MHz	3.0mN/m	0.054	1.42

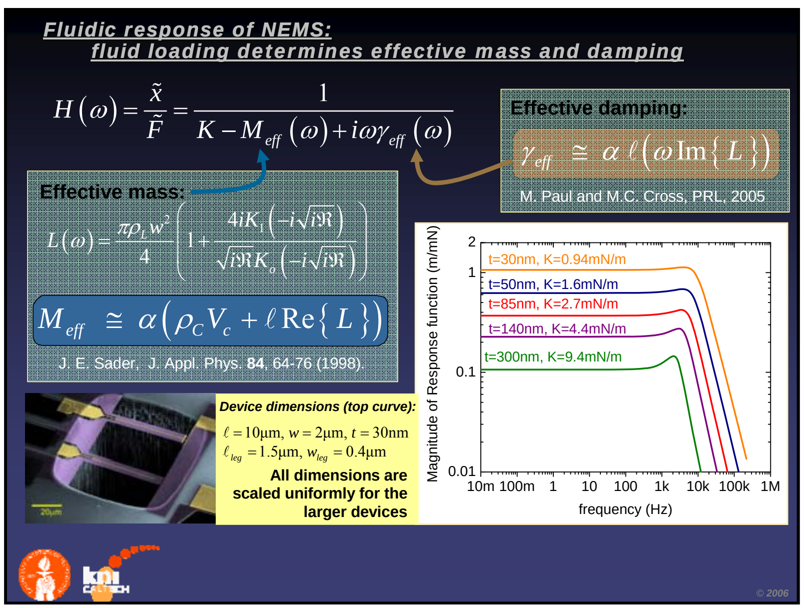

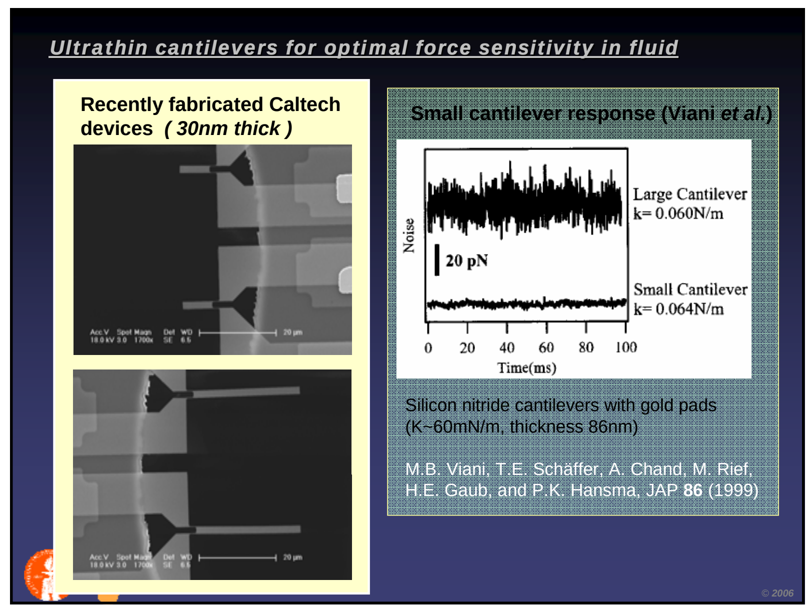

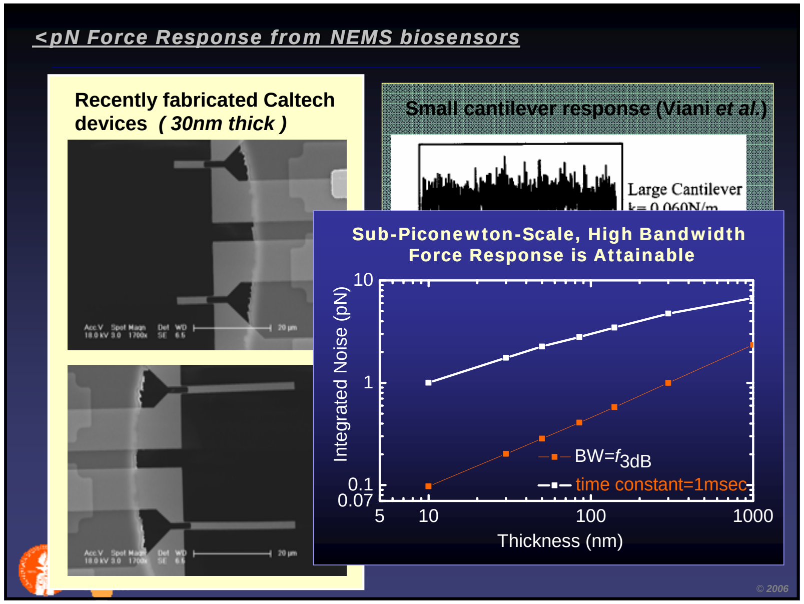
<pN Force Response from NEMS biosensors
Recently fabricated Caltech devices (30nm thick)
Small cantilever response (Viani et al.)
Large Cantilever
Sub-Piconewton-Scale, High Bandwidth Force Response is Attainable
Integrated Noise (pN)
Thickness (nm)
BW=f3dB
time constant=1msec
© 2006

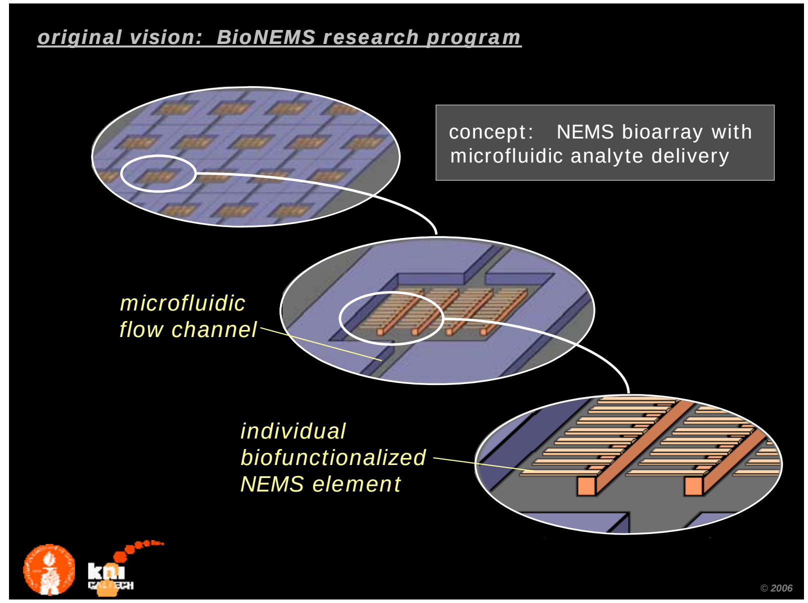
original vision: BioNEMS research program
concept: NEMS bioarray with microfluidic analyte delivery
microfluidic flow channel
individual biofunctionalized NEMS element
© 2006

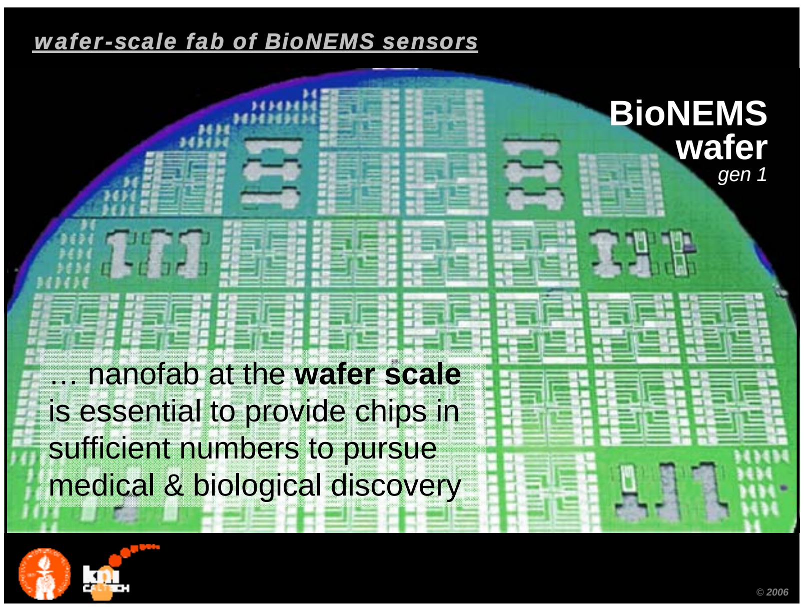
wafer-scale fab of BioNEMS sensors
BioNEMS wafer
gen 1
… nanofab at the wafer scale is essential to provide chips in sufficient numbers to pursue medical & biological discovery
© 2006

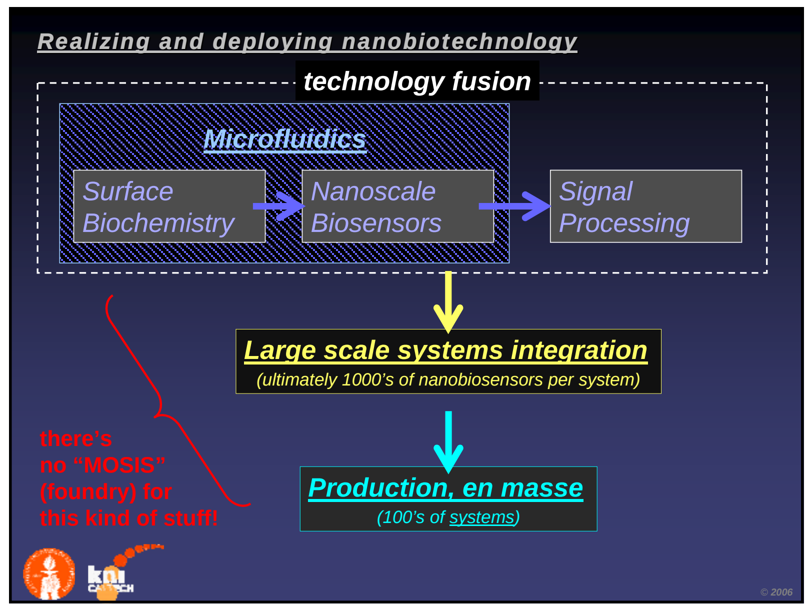
Realizing and deploying nanobiotechnology
technology fusion
Microfluidics
Surface Biochemistry
Nanoscale Biosensors
Signal Processing
Large scale systems integration
(ultimately 1000's of nanobiosensors per system)
Production, en masse
(100's of systems)
there's no "MOSIS" (foundry) for this kind of stuff!
© 2006

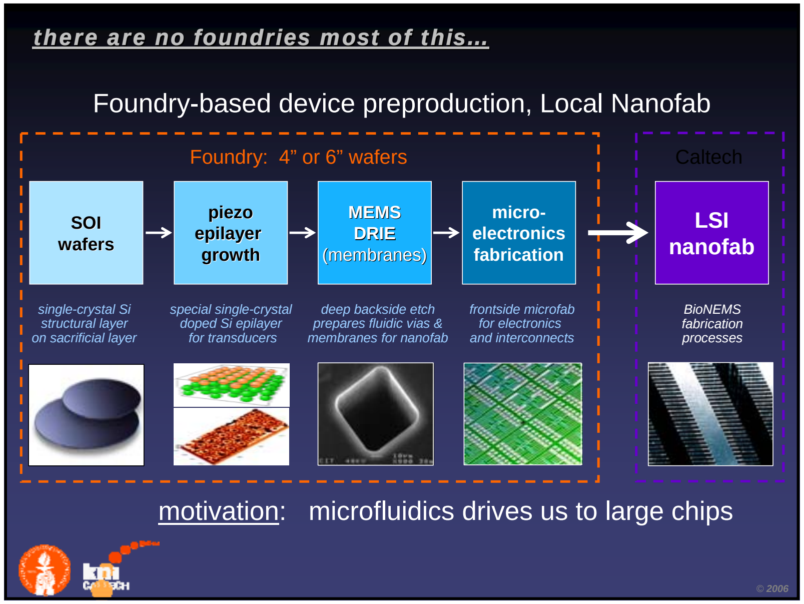
there are no foundries most of this...
Foundry-based device preproduction, Local Nanofab
Foundry: 4" or 6" wafers
Caltech
SOI wafers
piezo epilayer growth
MEMS DRIE (membranes)
micro-electronics fabrication
LSI nanofab
single-crystal Si structural layer on sacrificial layer
special single-crystal doped Si epilayer for transducers
deep backside etch prepares fluidic vias & membranes for nanofab
frontside microfab for electronics and interconnects
BioNEMS fabrication processes
motivation: microfluidics drives us to large chips
© 2006

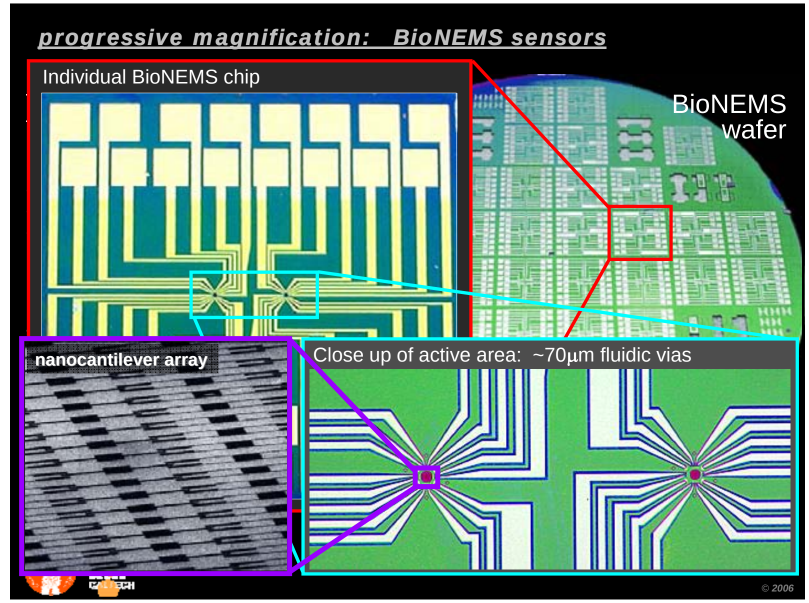
progressive magnification: BioNEMS sensors
Individual BioNEMS chip
BioNEMS wafer
nanocantilever array
Close up of active area: ~70µm fluidic vias
© 2006

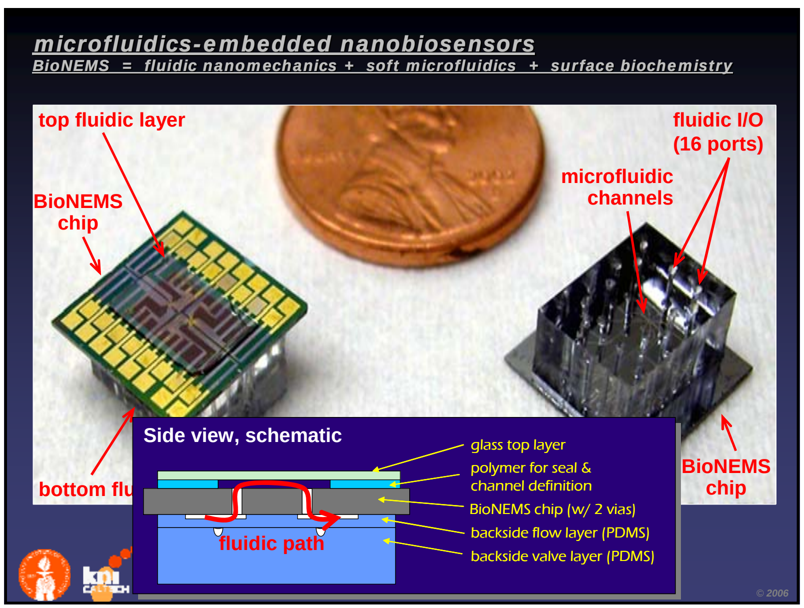
microfluidics-embedded nanobiosensors
BioNEMS = fluidic nanomechanics + soft microfluidics + surface biochemistry
top fluidic layer
BioNEMS chip
fluidic I/O (16 ports)
microfluidic channels
bottom flu
Side view, schematic
glass top layer
polymer for seal & channel definition
BioNEMS chip (w/ 2 vias)
backside flow layer (PDMS)
backside valve layer (PDMS)
fluidic path
BioNEMS chip
© 2006

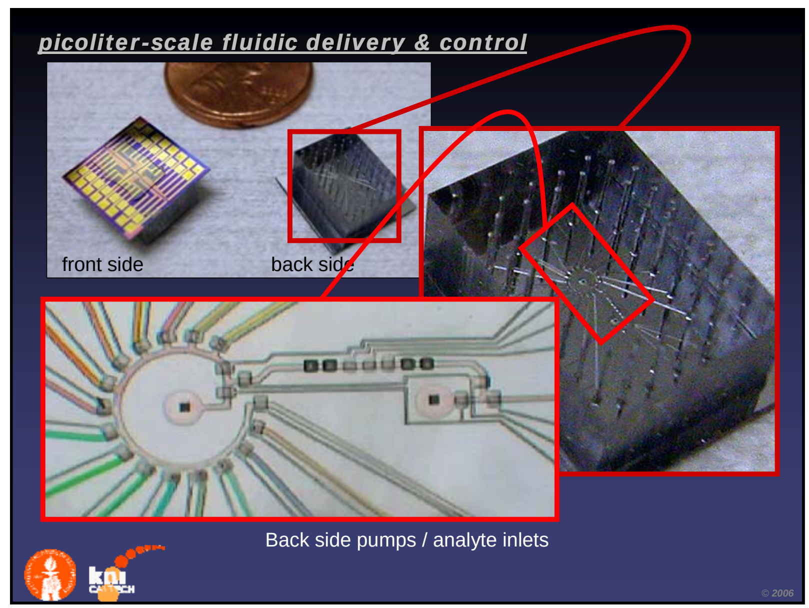
picoliter-scale fluidic delivery & control
front side
back side
Back side pumps / analyte inlets
© 2006

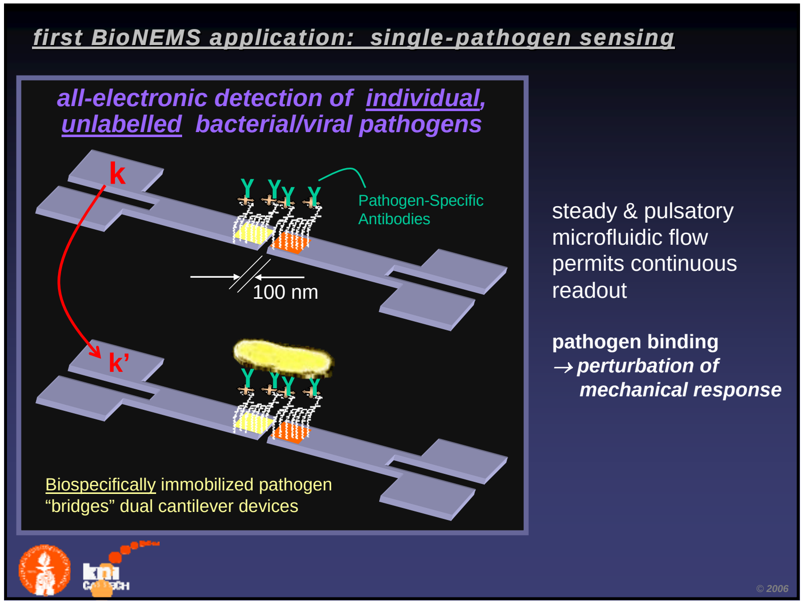
first BioNEMS application: single-pathogen sensing
all-electronic detection of individual, unlabelled bacterial/viral pathogens
k
Pathogen-Specific Antibodies
100 nm
k'
Biospecifically immobilized pathogen "bridges" dual cantilever devices
steady & pulsatory microfluidic flow permits continuous readout
pathogen binding
→ perturbation of mechanical response

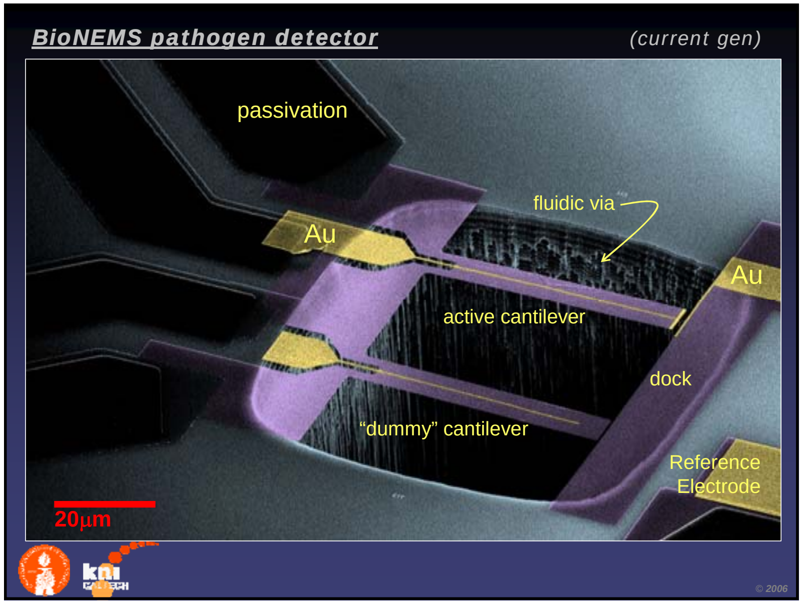
BioNEMS pathogen detector
(current gen)
passivation
fluidic via
Au
Au
active cantilever
dock
"dummy" cantilever
Reference Electrode
20μm

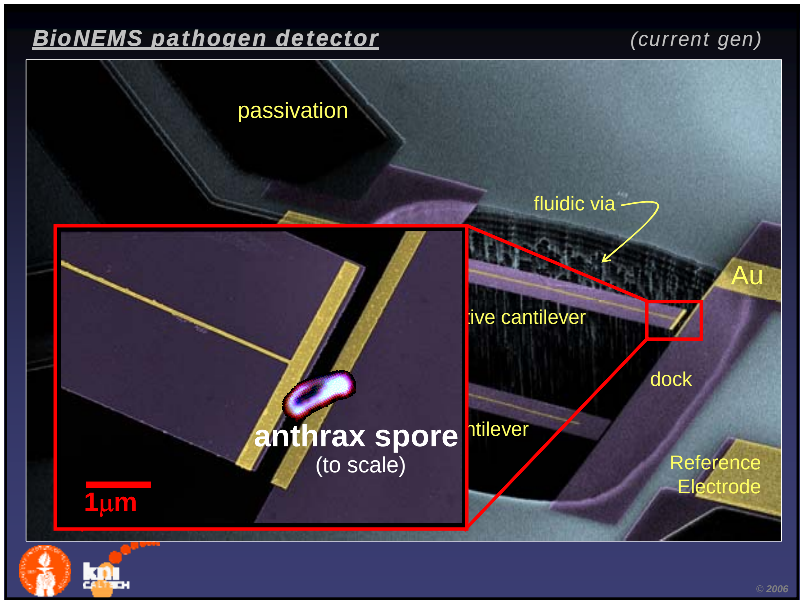
BioNEMS pathogen detector
(current gen)
passivation
fluidic via
Au
tive cantilever
dock
ntilever
Reference Electrode
anthrax spore
(to scale)
1μm

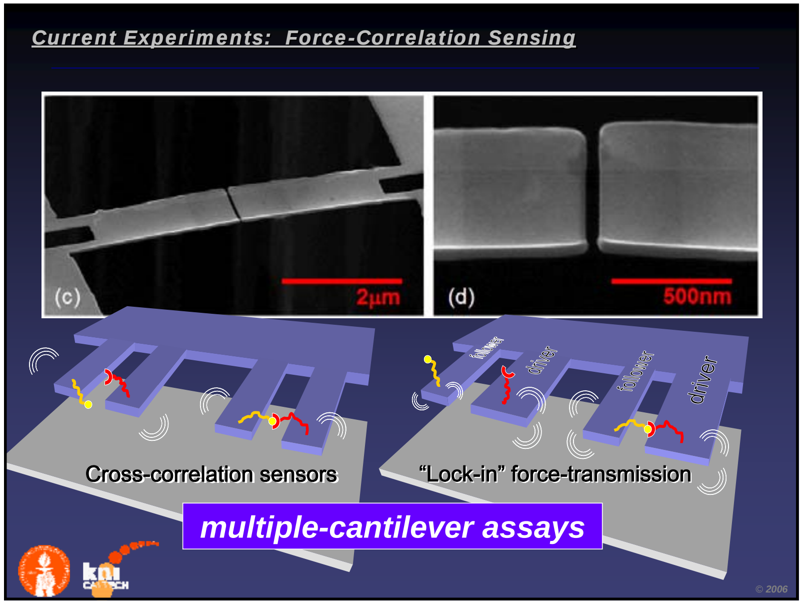
Current Experiments: Force-Correlation Sensing
(c)
2μm
(d)
500nm
Cross-correlation sensors
"Lock-in" force-transmission
driver
driver
multiple-cantilever assays

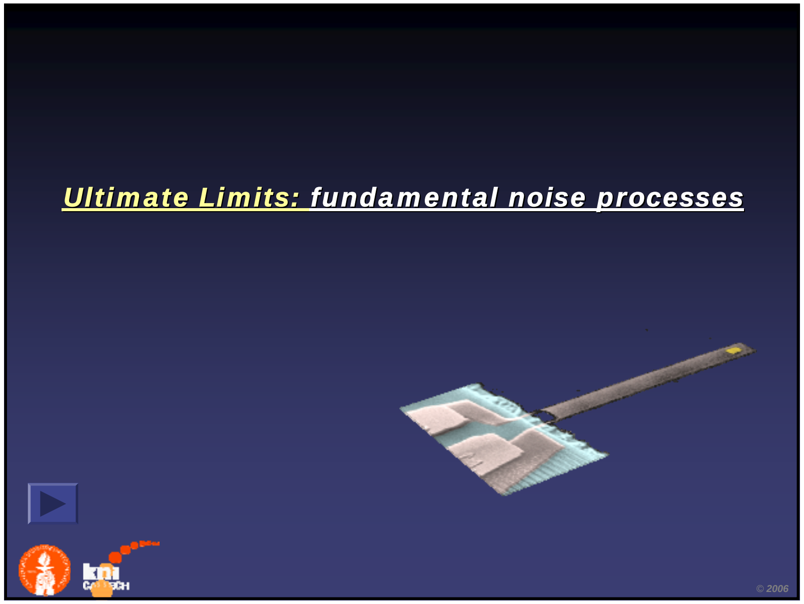
Ultimate Limits: fundamental noise processes
© 2006

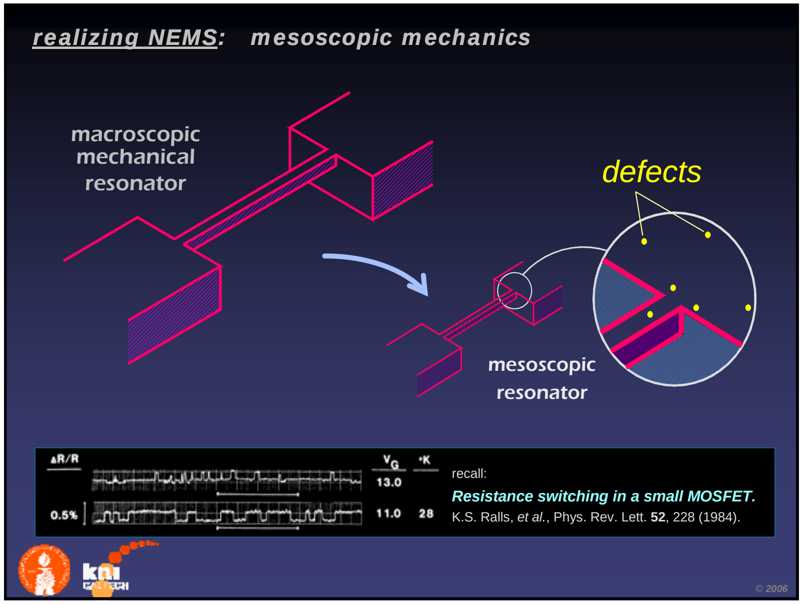
realizing NEMS: mesoscopic mechanics
macroscopic mechanical resonator
defects
mesoscopic resonator
ΔR/R
0.5%
V_G
13.0
11.0
°K
28
recall:
Resistance switching in a small MOSFET.
K.S. Ralls, et al., Phys. Rev. Lett. 52, 228 (1984).
© 2006

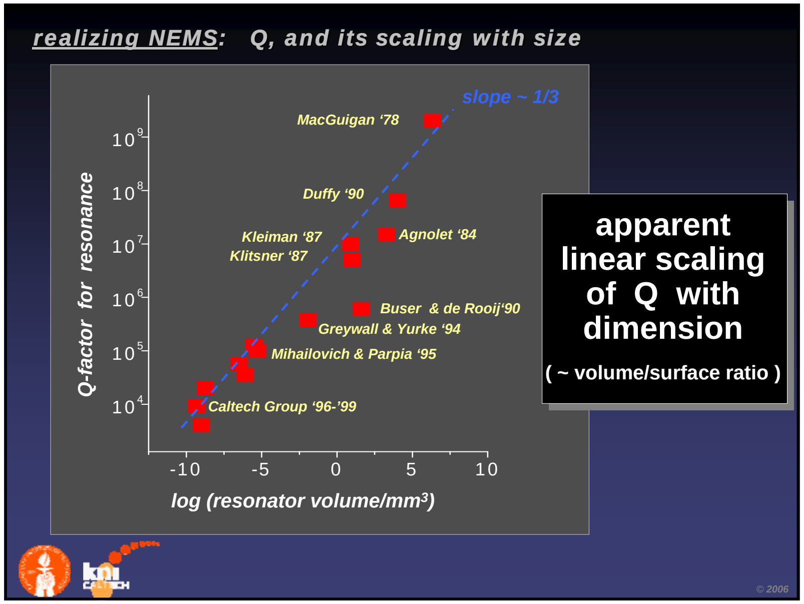
realizing NEMS: Q, and its scaling with size
slope ~ 1/3
MacGuigan '78
Duffy '90
Kleiman '87
Klitsner '87
Agnolet '84
Buser & de Rooij'90
Greywall & Yurke '94
Mihailovich & Parpia '95
Caltech Group '96-'99
Q-factor for resonance
10^9
10^8
10^7
10^6
10^5
10^4
-10
-5
0
5
10
log (resonator volume/mm³)
apparent linear scaling of Q with dimension
(~ volume/surface ratio)
© 2006

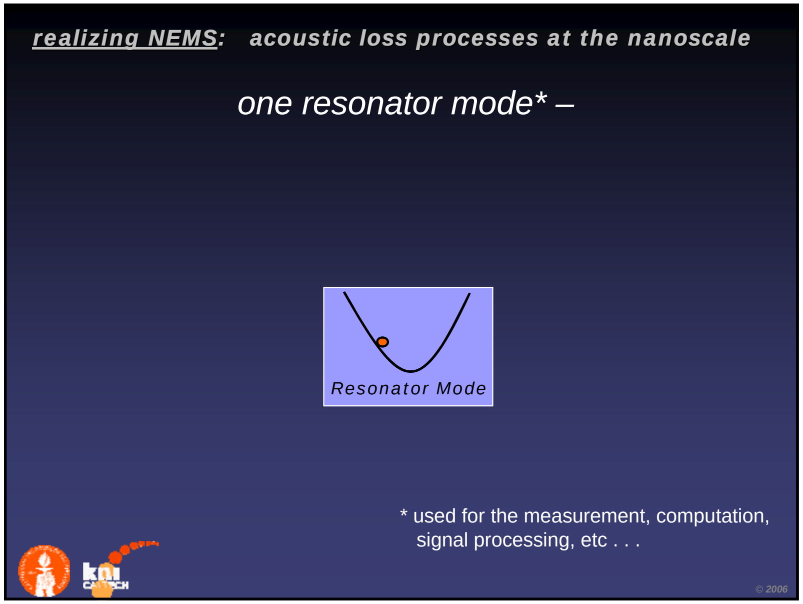
realizing NEMS: acoustic loss processes at the nanoscale
one resonator mode* –
Resonator Mode
* used for the measurement, computation, signal processing, etc . . .
© 2006

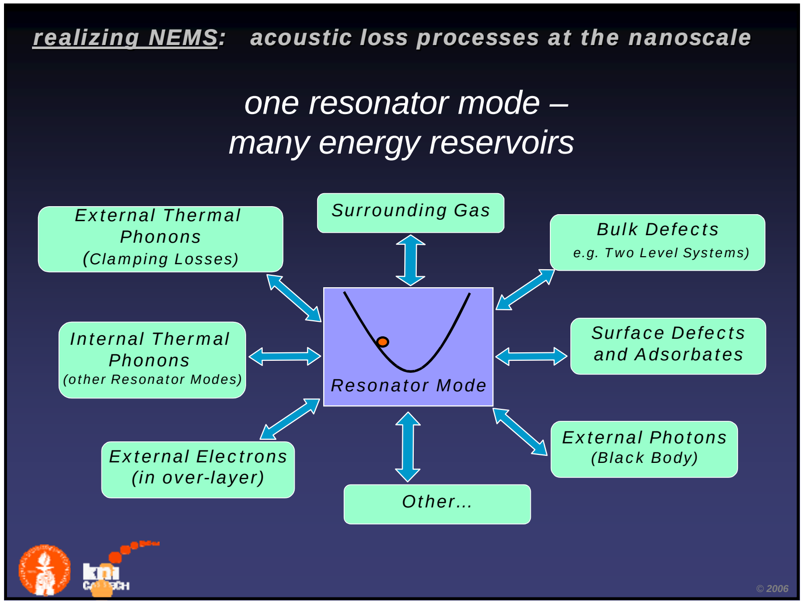

(some) references

(NOTE: many of the references on this page can be found on-line at: http://nano.caltech.edu/publicat.html)

- **Fundamentals, beam theory, etc.**

  A. N. Cleland, *Fundamentals of Nanomechanics* (Springer-Verlag, Heidelberg, Germany, 2002).

- **Introductory Reviews**

  M.L. Roukes, *"Nanoelectromechanical Systems"*, Opening Lecture, 2000 Solid State Sensor and Actuator Workshop, Hilton Head, SC 6/4/2000, published in "Technical Digest of the 2000 Solid State Sensor and Actuator Workshop" (Transducers Research Foundation, Cleveland, OH; 2000) ISBN 0-9640024-3-4; on-line at: http://www.arxiv.org/pdf/cond-mat/0008187

  Ekinci KL, Roukes ML, *"Nanoelectromechanical systems"*, Review of Scientific Instruments 76 061101 JUN 2005

  Roukes ML, *"Plenty of Room Indeed"*, SCIENTIFIC AMERICAN 285: (3) 48-57 SEP 2001

  Roukes M, *"Nanoelectromechanical systems face the future"*, PHYSICS WORLD 14: (2) 25-31 FEB 2001

- **Noise in NEMS**

  Cleland AN, Roukes ML, *"Noise processes in nanomechanical resonators"*, J APPL PHYS 92 (5): 2758-2769 SEP 1 2002

  Ekinci KL, Yang YT, Roukes ML, *"Ultimate limits to inertial mass sensing based upon nanoelectromechanical systems"*, J. Appl. Phys. 95 2682 MAR2004

- **NEMS Transduction / Actuation**

  K.L. Ekinci, *"Electromechanical Transducers at the Nanoscale: Actuation and Sensing of Motion in Nanoelectromechanical Systems (NEMS)"*, Small 2005, 1, No. 8-9, 786 –797; on-line at http://nanoscience.bu.edu/papers/Ekinci%20review.pdf

- **Quantum Limits**

  Schwab KC, Roukes ML, *"Putting Mechanics into Quantum Mechanics"*, Physics Today JULY 2005 on-line at: http://nano.caltech.edu/papers/Schwab-Roukes-PT-July05.pdf